Transcriptional responses of *Escherichia coli* during recovery from inorganic or organic mercury exposure

Stephen LaVoie (slavoie5@uga.edu) and Anne O. Summers* (summers@uga.edu)

Department of Microbiology, University of Georgia, Athens, Georgia 30602

Keywords: longitudinal RNA-Seq, transcriptomics, toxic metals, essential metals, stress response, biofilm, phenylmercury, antibiotic resistance

ABSTRACT

Background: The protean chemical properties of mercury have long made it attractive for diverse applications, but its toxicity requires great care in its use, disposal, and recycling. Mercury occurs in multiple chemical forms, and the molecular basis for the distinct toxicity of its various forms is only partly understood. Global transcriptomics applied over time can reveal how a cell recognizes a toxicant and what cellular subsystems it marshals to repair and recover from the damage. The longitudinal effects on the transcriptome of exponential phase *E. coli* were compared during sub-acute exposure to mercuric chloride ($HgCl_2$) or to phenylmercuric acetate (PMA) using RNA-Seq.

Results: Differential gene expression revealed common and distinct responses to the mercurials throughout recovery. Cultures exhibited growth stasis immediately after each mercurial exposure but returned to normal growth more quickly after PMA exposure than after $HgCl_2$ exposure. Correspondingly, PMA rapidly elicited up-regulation of a large number of genes which continued for 30 min, whereas fewer genes were up-regulated early after $HgCl_2$ exposure only some of which overlapped with PMA up-regulated genes. By 60 min gene expression in PMA-exposed cells was almost indistinguishable from unexposed cells, but $HgCl_2$ exposed cells still had many differentially expressed genes. Relative expression of energy production and most metabolite uptake pathways declined with both compounds, but nearly all stress response systems were up-regulated by one or the other mercurial during recovery.

Conclusions: Sub-acute exposure influenced expression of ~45% of all genes with many distinct responses for each compound, reflecting differential biochemical damage

by each mercurial and the corresponding resources available for repair. This study is the first global, high-resolution view of the transcriptional responses to any common toxicant in a prokaryotic model system from exposure to recovery of active growth. The responses provoked by these two mercurials in this model bacterium also provide insights about how higher organisms may respond to these ubiquitous metal toxicants.

BACKGROUND

The common metallic element mercury (Hg) has no beneficial biological function and its chemical similarities to essential transition metals such as zinc, copper, and iron make it highly toxic to all living systems. Global mercury emissions range from 6500 to 8500 Mg annually with estimates of half [1, 2] and even two-thirds [3] being anthropogenic and the rest from volcanism. Mercury exists in multiple chemical forms that are readily susceptible to abiotic and biotic inter-conversions [4]. Mercury occurs naturally as the insoluble HgS ore (cinnabar), as inorganic complexes of Hg^{+2}, Hg^{+1}, or $(Hg_2)^{2+}$ of varying solubility depending on available ligands, and as organomercurials generated by microbial and anthropogenic processes.

Major sources of chronic mercury exposure in humans include dental amalgam fillings [5, 6], consumption of fish containing methylmercury [7], and artisanal gold mining operations [8]. Organomercurials, like phenylmercury, methylmercury, and merthiolate (ethylmercury) have historically been used in medical, industrial and agricultural applications as antimicrobial or fungicidal agents [9-11]. The toxic effects of mercury exposure in humans are associated with neurological, kidney, liver, gastrointestinal, and developmental disorders [9, 12-15].

70 Like other common electrophilic toxic metals such as arsenic, cadmium, and
71 lead, there is no single biochemical target for mercury damage. Mercury has a strong
72 affinity for sulfur and selenium [16, 17] and therefore targets the cellular thiol pool,
73 composed of glutathione and cysteine thiol groups of proteins [9] and selenocysteine, a
74 rare but critical amino acid in proteins involved in redox defense and thyroid function
75 [18]. Depletion of the cellular thiol pool and disruption of the cellular membrane potential
76 by mercury can induce oxidative stress and apoptosis pathways in mitochondria [19,
77 20]. However, there is no evidence that mercury itself undergoes Fenton-type chemistry
78 to generate reactive oxygen species like iron and copper [21].
79 In earlier work we used global proteomics to identify stable mercury-protein
80 binding sites in growing *E. coli* cells exposed to acute levels of organic or inorganic Hg
81 [22]. We found cysteine sites in several hundred proteins, many highly conserved
82 evolutionarily, that formed stable adducts with one or more of these mercurials,
83 consequently disrupting many cellular processes such as iron homeostasis and the
84 electrolyte balance [23]. Importantly, we found that organic and inorganic mercurials
85 had distinct effects on these cellular processes and distinct protein structural
86 preferences. Although the pathobiology of organic and inorganic mercurials has been
87 known for decades to differ, with methyl- and ethyl-mercury recognized as neurotoxic
88 and inorganic mercury as neurotoxic, nephrotoxic, hepatotoxic, and immunotoxic, no
89 previous studies at that time had assessed the biochemical underpinnings of these
90 distinctions on a global scale in any model system.
91 Motivated by our proteomics observations and by microarray data from *C.*
92 *elegans* showing distinct transcriptional single end point response and toxicity for

93 inorganic and organic mercurials [24], we applied RNA-Seq to examine the
94 transcriptional effects of $HgCl_2$ and phenylmercuric acetate (PMA) exposure on *E. coli*
95 K-12 MG1655 over time. This is the first study to examine the global transcriptional
96 response to mercury exposure in a microorganism and the only study to compare
97 directly the effects of different compounds over time through recovery. The changes in
98 gene expression were idiosyncratic for each compound, confirming and extending the
99 idea that the cell suffers overlapping but distinct biochemical damage and marshals
100 both distinct and overlapping recovery processes in response to these chemically
101 distinct mercurials. Although our work was in a bacterium, the high evolutionary
102 conservation of many of the genes whose expression we identified as mercury-
103 vulnerable offers insights for the toxicology of mercury compounds in higher organisms.
104

105 **METHODS**

106 ***Cell cultures.***

107 For each biological RNA-Seq replicate *E coli* K-12 MG1655 was subcultured from
108 cryostorage on Luria-Bertani (LB) agar overnight at 37°C. A half-dozen well-isolated
109 colonies were used to inoculate a 20 ml starter culture in Neidhardt MOPS Minimal
110 Medium (NM3) [25] (0.2% final glucose concentration) supplemented with 20 mg/L
111 uracil and 500 µg/L thiamine, which was incubated at 37°C with shaking at 250 rpm
112 overnight (~18 hr). The overnight starter culture was diluted 1:30 to initiate the
113 experimental culture and divided into three 500 ml flasks with 100 ml NM3 in each,
114 which were incubated at 37°C with shaking at 250 rpm. When cultures reached $OD_{595} \approx$
115 0.470 (~ 200 min), two cultures were made 3 µM mercuric chloride ($HgCl_2$) or 3 µM

116 phenylmercuric acetate (PMA) and the third was left as an unexposed control. Mercury
117 stocks were prepared fresh for each growth experiment: 10 mM $HgCl_2$ (Fisher) in water
118 and 5 mM PMA (Sigma) in 25% dimethyl sulfoxide DMSO (Fisher), which is 2.1 mM or
119 0.015% v/v final concentration DMSO in culture. These mercurial exposures were
120 chosen from prior pilot experiments to find exposure conditions (OD_{595}, mercurial
121 concentration and sampling times) that displayed a marked decrease in growth rate
122 relative to the unexposed control but allowed subsequent restoration of rapid growth
123 rate (i.e. recovery) within 1 hr (approximately one generation in NM3) after mercurial
124 exposure. Duplicate 1-ml aliquots of each culture were collected at 0 (unexposed
125 control only), 10, 30, 60 min after mercurial exposure and immediately centrifuged at
126 20,800 *x g* for 3 min at 4°C. Spent medium was aspirated and cell pellets were frozen at
127 -70°C within 5 min after collection. Seven biological replicates were prepared following
128 this protocol and the average variance for all replicates in culture optical density over
129 each 90-min experiment ranged from 0.0019 – 0.0073. The three biological replicates
130 with the lowest variance between growth curves (range from 0.0007 – 0.0017 for all
131 time points) were prepared for RNA-Seq.
132
133 ***Purification of mRNA***
134 One cell pellet from each condition and sampling time was thawed on ice for all
135 three biological replicates; total RNA was isolated by RNA*snap*™ [26] and stored at -
136 70°C. DNA contamination was removed by two treatments with Turbo-DNase (Ambion;
137 Life Technologies). RNA concentrations and A_{260}/A_{280} ratios were determined using a
138 Nanodrop™ 1000 spectrophotometer (Thermo Scientific). Ribosomal RNA depletion was

139 performed with the Ribo-Zero™ rRNA removal kit for Gram-negative bacteria (Epicentre)
140 and concentrated using RNA Clean and Concentrator™ -5 columns (Zymo Research)
141 following the manufacturer's instructions. Purified mRNA was quantified using the
142 Nanodrop™ and stored at -70°C.
143
144 ***Library Preparation and Next-generation Sequencing***
145 The quality and quantity of rRNA-depleted RNA was assessed on a 2100
146 Bioanalyzer RNA pico chip (Agilent Technologies) using the manufacturer's
147 recommendations. Next-generation sequencing (NGS) libraries were prepared using the
148 Kapa biosystems NGS stranded library prep kit for RNA-Seq with dual indexed Illumina
149 adapters. Library insert size was ~150 bp, as determined by high-sensitivity NGS
150 fragment analysis kit for Fragment Analyzer™ (Advanced Analytical Technologies) using
151 the manufacturer's instructions. Quantification of each library was done by qPCR and all
152 30 libraries were pooled in equal concentrations. The library preparation, quality
153 analysis, and pooling were performed by the Georgia Genomics Facility
154 (http://dna.uga.edu). Paired-end (2 x 50 bp) sequencing of the pooled libraries using the
155 Illumina HiSeq 2000 platform was performed by the HudsonAlpha Institute for
156 Biotechnology Genomic Services Laboratory (http://gsl.hudsonalpha.org). See Table S1
157 for index and filename information for data uploaded to NCBI Gene Expression
158 Omnibus database (http://www.ncbi.nlm.nih.gov/geo/) with accession ID: GSE95575.
159
160 ***Data Processing and Differential Expression Analysis***

161 Quality control processing of sequence data was performed using Galaxy
162 (https://galaxyproject.org) on the Georgia Advanced Computing Resource Center at the
163 University of Georgia. The FASTX tools in Galaxy
164 (http://hannonlab.cshl.edu/fastx_toolkit) were used for filtering by quality (80% of
165 sequence ≥ quality score of 20), then reads were trimmed at both 5' and 3' ends using a
166 window and step size of 1 with quality score ≥ 20. Forward- and reverse-read mate-
167 pairs were assembled and aligned to the *Escherichia coli* MG1655 K-12 genome using
168 Bowtie2 [27]. SAMtools [28] was used to convert Bowtie2 output (.bam file) to SAM
169 format. The number of sequence reads that aligned to features in the annotation file
170 (Escherichia_coli_str_k_12_substr_mg1655.GCA_000005845.2.24.gtf from
171 http://bacteria.ensembl.org) were tabulated from the resulting SAM alignment files using
172 the HTSeq-count program [29] with intersection non-empty mode. Mapped read counts
173 were analyzed for significant differential expression (false discovery rate of ≤ 0.01, fold-
174 change ≥ 2) using the baySeq package in R [30]. All genes that did not meet both the ≤
175 1% FDR and ≥ 2 fold-change criteria were indicated as no-change in figures, tables,
176 and text. Within baySeq, two-way comparisons using quantile normalization were made
177 for all three biological replicate transcriptomes over time for $HgCl_2$ exposure or PMA
178 exposure versus the unexposed control. We also examined changes over time in the
179 unexposed control culture itself.
180

181 **RESULTS**

182 ***Effects of sub-acute mercury exposure on growth of MG1655.***

183 We defined sub-acute exposure as the concentration of mercury that clearly
184 inhibited growth relative to the unexposed control but allowed cells to resume growth
185 within 1 hour or approximately one generation in this medium (Figure 1a, Figure S1).
186 We chose restoration of growth rate, not stationary phase cell density, as the
187 benchmark for recovery so as not to conflate normal cellular stationary phase "stop
188 growing" signals with mercury-induced "stop growing" signals. Based on pilot
189 experiments the appropriate dose proved to be 3 μM for both mercurials. Exposure to 4
190 - 5 μM $HgCl_2$ prevented growth resumption during 1 hr and the effects of PMA exposure
191 were similar at 3 and 5 μM; exposure to 2.5 μM of either mercurial did not consistently
192 retard growth (data not shown).
193 Cell-associated Hg (Table S2 and Supporting Information Methods) declined
194 slowly as has been reported previously for low level $HgCl_2$ exposure of Hg sensitive
195 cells and was attributed to non-specific endogenous reductants [31-33]. Bound Hg in
196 cells exposed either to $HgCl_2$ or to PMA declined similarly from ~50% of total Hg added
197 to culture at 10 min to ~20% at 30 min, after which Hg loss from PMA-exposed cells
198 continued to decline to 11% of input at 60 min. In contrast, cell-associated Hg in cells
199 exposed to $HgCl_2$ increased from 24% at 30 to 47% at 60 min. Presently, we have no
200 simple explanation for this unexpected difference in cell-bound Hg in late exponential
201 phase cultures, however it does echo our finding that cultures acutely exposed to 40 μM
202 or 80 μM PMA or $HgCl_2$ bound 24% or 208% more Hg(II) than PhHg, respectively [23].
203 Also notable was a brief drop in the culture optical density immediately after PMA
204 exposure consistent with some cell lysis as has been reported [34]. The lack of

205 apparent lysis after divalent $HgCl_2$ exposure may be due to its ability to cross-link cell
206 envelope proteins via their cysteines, which is not possible for monovalent PMA.
207
208 ***Transcriptome benchmarks***
209 Paired-end libraries averaged over 9.5 million reads and mapped reads provided
210 an average of 143X coverage (Figure S2). The sequencing data were of high quality,
211 requiring removal of only 11% as low-quality reads. Of the high-quality reads, 97% of
212 reads mate-paired, 99.4% of paired reads mapped to the genome and 82% of reads
213 mapped to an annotated genome feature on average from all libraries.
214 Overall 89% of annotated mapped reads were to coding regions (CDS) based on
215 raw un-normalized read counts per gene output from HTseq-count program [29](Figure
216 S3, Table S3, Table S4). Pearson correlations of raw read counts confirmed that no
217 strong biases were introduced in biological replicates for each condition (Figures S4-
218 S6). That dispersion is slightly greater in both mercury exposure conditions than in
219 unexposed cultures, especially at later time points, is consistent with perturbations of
220 multiple cellular processes.
221 Mapped reads to rRNA constituted only 0.3% of total reads (std. dev. = 0.425) on
222 average for all libraries (Table S3) consistent with effective Ribo-Zero™ rRNA removal.
223 In the unexposed culture non-coding RNA's (ncRNA) were 4% of total reads over all
224 time points, but their percentage increased in mercury exposure conditions indicating
225 greater differential expression of some ncRNA genes (details below). The very
226 abundant tmRNA (*ssrA*) needed for rescuing stalled ribosomes [35] was 6% of total
227 reads in the unexposed condition and although this percentage increased for mercury

228 exposure conditions, the tmRNA gene (*ssrA*) was not differentially expressed under any
229 condition. Pseudogenes accounted for less than 1% of total reads, but up to 35%
230 ($HgCl_2$) and 13% (PMA) of them were significantly up-regulated. The tRNA's were less
231 than 1% of total reads because the library preparation method we used was not
232 optimized for such small RNAs. However, approximately 35% of these observed tRNA
233 genes were significantly down-regulated during the first 30 min after exposure to either
234 mercurial.
235
236 ***$HgCl_2$ and PMA transcriptional responses are not the same.***
237 We expected that significantly differentially expressed genes (DEGs) in the
238 mercury exposure conditions (compared to the unexposed cells) would change over
239 time as the cells transitioned from initial growth stasis back into a normal growth rate.
240 We also expected that some DEG responses would be similar because both mercurials
241 are thiophilic and will bind to the cellular thiol redox buffer, glutathione (GSH), and to
242 protein cysteine residues. However, since there are physiological differences and
243 protein site preferences for each compound in acute Hg(II)- or PMA-exposure [23 and
244 Zink et. al. in preparation] we aimed here at a low exposure using a longitudinal protocol
245 to discern more subtle distinctions between these mercurials as the cells experienced
246 stasis and then recovered their growth rate. In the following sections, we first describe
247 the bulk measures of gene expression over time and then describe differences in
248 specific functional pathways.
249
250 ***Differentially expressed genes: the view from 30,000 feet.***

251 *(a) Differentially expressed genes (DEG) for each condition and time point*

252 DEGs were determined by pairwise comparisons of mercury exposure conditions
253 relative to the unexposed culture at the corresponding time point (Figure 1b and Table
254 S5). Ten minutes after exposure, expression of 41% or 49% of the 4,472 non-rRNA
255 genes changed significantly for $HgCl_2$ or PMA-exposed cells, respectively (Figure 1b).
256 At 30 min with growth still arrested, 32% of genes in the $HgCl_2$-exposed cells were
257 differentially expressed (Figure 1b), (Figure 1a, red). In contrast, PMA-exposed cells at
258 30 min began to recover their prior growth rate (Figure 1a, green), but 45% of their
259 genes remained differentially expressed (Figure 1b). By 60 min, the PMA-exposed cells
260 were growing at nearly their pre-exposure rate and only 1.5% of genes were
261 differentially expressed, whereas the $HgCl_2$-exposed cells were still growing more
262 slowly than pre-exposure with 13% of their genes still differentially expressed compared
263 to the unexposed cells (Figure 1b).

264

265 *(b) Shared and unique genes at each time point for each exposure.*

266 The total distinct DEGs across all time points was slightly lower for $HgCl_2$ (2,327)
267 than for PMA (2,541) exposure (Figure 1b and Figure S7). More striking were the
268 differences in DEGs at each time point; PMA-exposed cells modulated 20% more genes
269 at 10 min (2,181 vs 1,821) and 40% more at 30 min (2,007 vs 1,422) than $HgCl_2$
270 exposed cells. This trend completely reversed by 60 min when DEGs declined in both
271 exposure conditions but $HgCl_2$ exposed cells were still modulating ~9-fold more genes
272 (563) than PMA-exposed cells (65), consistent with the latter recovering normal growth
273 sooner (Figure 1a). Also notable is the carryover of DEGs from one time point to the

274 next where $HgCl_2$ exposed cells have 1,001 DEGs in common at 10 and 30 min after
275 exposure but that number is 65% greater in PMA-exposed cells (1,650) (Figure S7).
276 However, $HgCl_2$ exposed cells have 52% more DEGs that are unique at 10 min
277 compared to PMA-exposed cells (804 vs 529), i.e. more $HgCl_2$ provoked DEGs occur
278 sooner after exposure than later. $HgCl_2$ exposure also yields more DEGs that occur at
279 all time points compared to PMA (Figure S7) since there are very few DEGs at 60 min
280 for PMA exposure.
281
282 *(c) Up-regulated vs. down-regulated genes for each exposure*
283 Sorting expression simply into genes up-regulated or down-regulated by $HgCl_2$ or
284 PMA at each time point (Figure 2) revealed additional quantitative distinctions between
285 them. For up-regulated genes, PMA-provoked more unique DEGs than DEGs in
286 common with $HgCl_2$ exposure at all time points, in contrast to $HgCl_2$ which had more
287 DEGs in common than unique at all but the last time point. This trend was not continued
288 for down-regulated genes where more genes were in common for both compounds than
289 unique at all time points.
290 Thus, early in exposure the cell reduced expression of a similar number of genes
291 for both mercurials, but up-regulated expression of many more genes in response to
292 PMA than to $HgCl_2$, and these distinct trends persisted to the middle time point. By 60
293 min, gene expression of PMA-exposed cells closely resembled that of unexposed cells,
294 but $HgCl_2$ exposed cells still have many up- and down-DEGs, consistent with slower
295 growth rate recovery by $HgCl_2$ exposed compared to PMA-exposed cells (Figure 1a).
296

297 *(d) Differentially expressed genes grouped by functional category.*

298 To sort our observations from a different perspective, the DEGs for each
299 condition were grouped by Clusters of Orthologous Groups (COGs) to identify
300 expression differences based on gene functions (Figure 3 and Table S6). For most
301 COGs, both mercurials elicited their strongest responses, up- or down-regulated, within
302 the first 10 min of exposure (Figure 3); in most cases, the responses were of similar
303 magnitude. At 30 min, the PMA (green) responses remained nearly the same, up- or
304 down-regulated, but $HgCl_2$ provoked responses (red) generally diminished, often
305 sharply. By 60 min, expression in PMA-exposed cells was barely distinguishable from
306 the unexposed cells in all COG categories, whereas $HgCl_2$ exposed cells had notable
307 differential expression in most COG categories.

308 The four well-defined COG categories with the most DEGs were energy
309 production (C), amino acid metabolism (E), carbohydrate metabolism (G), and
310 transcription (K), which are also categories with a large number of genes (284, 355,
311 381, and 294 respectively) in *E. coli* (Figure 3 legend). COG categories R and S
312 encoding poorly defined (261) or non-defined (203) genes were also represented
313 proportionally. These data suggest both mercurials broadly affect most metabolic
314 categories, albeit to different degrees and at different rates. However, four well-defined
315 COG categories have strikingly different responses to $HgCl_2$ and PMA. COG categories
316 for nucleotide metabolism (F), translation (J), motility (N), and intracellular trafficking (U)
317 have many fewer up-regulated genes in $HgCl_2$ exposed cells than in PMA-exposed
318 cells. There are relatively few DEGs involved in cell division (D), extracellular structures
319 (W), and mobile genetic elements (X) and genes within these categories responded

320 similarly to both mercurials. Thus, grouping DEGs by COGs illuminates the broad
321 functional differences and similarities between $HgCl_2$ and PMA exposure. Moreover, this
322 view makes clear that DEGs occur in all functional categories for both compounds, but
323 still display distinct differences in global transcriptional response to each compound. We
324 provide gene-level detail on several of these functional groups below. Note that the
325 COG database only includes functional annotations for 3,398 of *E. coli's* 4,497 genes,
326 but functional categories discussed below in more detail are not limited to COG-
327 annotated genes.

328 A heat map of the DEGs log-fold changes (Figure 4) provides a more granular
329 look at all DEGs for both compounds across all time points. The heat map, using Ward's
330 minimum variance clustering method [36], shows considerable uniformity of up- and
331 down-regulated expression during the 30 min after PMA exposure. In contrast, although
332 $HgCl_2$ exposed cells grossly shared many DEGs with PMA-exposed cells (Figure 2), the
333 heat map reveals a more variegated response to Hg(II) in which different genes are up-
334 or down-regulated at all time points, in contrast to the relatively consistent response of
335 PMA during recovery. Overall, 34% of DEGs are unique to only one mercurial and ~3%
336 of all DEGs had an opposite response to each compound (Table S5). The most
337 dramatic differences were at 60 min when $HgCl_2$ exposed cells were still modulating
338 many genes but PMA-exposed cells had only minor differences with unexposed cells,
339 consistent with their faster recovery of normal growth (Figure 1a). We dissect some of
340 these differences in function-specific heat maps below.

341 We also used STRING (version 10.0) [37, 38] for unsupervised network analysis
342 to identify gene clusters that were up-regulated in response to each compound (Figure

343 S8 and Table S7). We focused on up-regulated genes on the working assumption that
344 they are more likely to contribute to recovery than genes whose expression is turned
345 down. Gene clusters were generated by STRING based on organism specific data
346 mining to identify genes with a functional association, such as a common biological
347 purpose, location within the same operon, or shared regulatory mechanism. Note that
348 this network algorithm does not consider fold-change intensity of response; it
349 enumerates only whether an up-regulated gene is present at a given time point. The up-
350 regulated DEGs (nodes) of $HgCl_2$ exposed cells formed several tight clusters
351 encompassing 16 gene-ontology functions (GOFs) at 10 min, nine GOFs at 30 min, and
352 seven GOFs at 60 min (Figure S8 and Table S7). In contrast, although there were more
353 nodes for PMA-exposure at 10 and 30 min, there were fewer edges yielding no well-
354 defined clusters at 10 min and only two GOFs at 30 min. This network analysis
355 suggests that, although PMA provokes more DEGs than Hg(II) does, there is less
356 functional congruence between the genes involved in the response to PMA. Specific
357 gene and function changes are discussed further in the next section.

358 Lastly, as a control for using RNA-Seq in a longitudinal experiment, we observed
359 DEGs at sequential time points in the unexposed control culture (Figure S9 and Table
360 S8). As expected, changes were gradual over time with no more than 5% of the
361 genome being differentially expressed from one time point to the next. At the 60 min
362 time point, as the cells approached stationary phase 815 genes were differentially
363 expressed compared to mid-log (time 0). Sorting these DEGs by COGs (Figure S9) and
364 by STRING network analysis (Figure S10 and Table S7) showed, as expected, many
365 DEGs were consistent with normal transitioning from mid-log to late-log phase [39, 40].

366

367 ***Higher resolution view of expression differences in specific functional groups***

368 ***during recovery from exposure to $HgCl_2$ or PMA***

369 Taking the perspective that a toxicant is a kind of signaling molecule, we

370 considered differences in gene expression for the two Hg compounds to reflect how the

371 cell senses the biochemically distinct damage produced by these two metallo-

372 electrophiles as manifest by what tools the cell calls upon to restore its viability. A quick

373 snapshot of the great extent of these compound-specific differences can be seen in the

374 genes with a >20-fold increase in differential expression after $HgCl_2$ exposure (Table 1)

375 or PMA exposure (Table 2). Here we emphasize up-regulated genes on the working

376 assumption they could contribute directly or indirectly to repairing damage caused by

377 mercurial exposure. The 25 genes highly up-regulated by $HgCl_2$ (Table 1) are involved

378 in altering the cell surface, oxidative stress response and repair, protein chaperones,

379 metals homeostasis, and ribonucleotide reductase. The vestigial prophage genes likely

380 play no rescue role for the cell and were simply activated by generalized stress

381 responses and have large fold-change values due to repressed expression under

382 normal growth conditions. The corresponding PMA response echoed only 8 of these 25

383 $HgCl_2$ high-responders, and notably did not include the vestigial phage genes.

384 For PMA, the highly up-regulated genes are a distinct contrast to those for $HgCl_2$.

385 First, the maximum amplitude of the PMA-provoked differential expression is generally

386 much less than for Hg(II)-provoked high differential expression (Table 1), which could

387 reflect the lower uptake of PMA. Secondly, while 11 of the 17 PMA-provoked genes

388 were also on the $HgCl_2$ highly differential expression list, ion transport and antibiotic
389 resistance loci were more prominent with PMA and prophage genes were absent.
390 These two snapshot tables make the points that both mercurials generate broad,
391 but idiosyncratic, cellular responses. To place these "tips of many icebergs" in their
392 larger cellular context, we used heat maps and tables of subsets of functionally related
393 genes to discuss the differential effects of $HgCl_2$ and PMA on twelve canonical cellular
394 systems in the following sections.
395
396 i. INFORMATIONAL MACROMOLECULES
397 *(a) DNA replication, recombination and repair*
398 Of the 24 genes for initiation and maintenance, and termination of chromosome
399 replication, there were more genes down-regulated (8) than up-regulated (3) in
400 response to $HgCl_2$ and an equal number up- or down-regulated genes (7) in response to
401 PMA (Table S9). Of the 14 genes encoding the replicative polymerase holoenzyme, four
402 genes capable of translesion synthesis (*polB*, *dinB*, *umuCD*) were up-regulated more by
403 $HgCl_2$ exposure (Table S9), suggesting a greater degree of direct or indirect DNA
404 damage by $HgCl_2$ exposure. Of the 45 genes for repair and recombination proteins the
405 transcriptional response to each mercurial was very similar (11 up-regulated and 16
406 down-regulated for $HgCl_2$; 9 up-regulated and 18 down-regulated for PMA). But there
407 were repair genes unique to each compound: *xthA*, *uvrAB*, *mutM,* and *recN* were only
408 up-regulated by $HgCl_2$; and *mutH* and *mutY* were only up-regulated by PMA.
409 The *recA, recN,* and *xthA* DNA repair genes were ~~the most~~ highly up-regulated
410 (≥10 fold) in response only to $HgCl_2$. The *recA* gene, induced by double-strand DNA

411 breaks, serves multiple roles in DNA repair [41, 42]. Curiously, expression of *recBCD,*
412 which is needed for break repair, either did not change or declined compared to
413 unexposed cells for both mercurials. Expression of several genes involved in repair
414 (*recG*, *nth*, *hsdS*, and *mcrC*) were down-regulated by both compounds, but with larger
415 negative fold-changes for PMA than $HgCl_2$. Thus, the cells responded quickly to both
416 mercurials, but some distinct responses suggest these two compounds directly or
417 indirectly yield different kinds of DNA damage.
418
419 *(b) Transcription*
420 Of the core RNA polymerase (RNAP) genes only PMA-exposure increased
421 expression of a single gene *rpoZ* (ω subunit), but expression decreased in the
422 remaining *rpoABC* core genes (Table S10). $HgCl_2$ exposure did not change expression
423 of any RNAP core genes except for a transient 3-fold drop in *rpoA* at 30 min. Only one
424 of the five termination factors, the Rho-directed anti-terminator, *rof,* increased and did
425 so for both mercurials with PMA again provoking a greater response.
426 Genes for three sigma factors displayed increased expression upon exposure to
427 either mercurial, with *rpoH* (heat shock sigma factor) and *rpoS* (stationary phase and
428 stress response sigma factor) increasing more following PMA-exposure and *rpoD*
429 (housekeeping sigma factor) only increasing after $HgCl_2$ exposure. The effects of $HgCl_2$
430 or PMA exposure on the regulation of genes within each regulon controlled by *E. coli's*
431 seven sigma factors are tabulated in Table S11. Many genes are modulated
432 differentially by $HgCl_2$ or PMA-exposure, but no single sigma factor is uniquely
433 responsible for increases or decreases in responses to these two compounds.

434 Many of the 203 transcriptional regulators annotated in the RegulonDB (Table 3)
435 [43, 44] and the 1,723 genes they control were expressed differently with the two
436 mercurials (Table S12). PMA provoked up-regulation of more transcription factor genes
437 at 10 and 30 min than $HgCl_2$ exposure, but slightly fewer down-regulated regulators
438 (Table 3). Of all COG categories, transcription had the most up-regulated genes for both
439 mercurials (Figure 3 and Table S6). PMA up-regulated ~40% more transcription related
440 genes at 10 min and ~80% more genes at 30 min than $HgCl_2$. Six activators (*mhpR,*
441 *glcC, gadX, soxS, mlrA, phoB*) and three repressors (*mcbR, iscR, betI*) were up-
442 regulated at all times for $HgCl_2$, but *gadX* was the only activator gene up-regulated at all
443 times for both mercurials (Table S12). GadX is part of the RpoS regulon [45] and
444 activates the acid resistance system and multidrug efflux [46, 47]. Details of
445 transcription factors and their regulons are provided in Table S12.
446 Lastly, *E. coli* has 65 currently annotated (ASM584v2), small non-coding RNAs.
447 Although our RNA purification and library preparation methods were not optimized for
448 their enrichment, we observed differential expression for a number of them (Table S5,
449 feature type "ncRNA"). ncRNAs up-regulated for both mercurials are involved in
450 regulation of acid resistance (*gadY*), oxidative stress (*oxyS*), and multiple transporters
451 (*gcvB* and *sgrS*). In contrast, adhesion and motility (*cyaR*), and anaerobic metabolism
452 shift (*fnrS*) were down-regulated by both compounds.
453
454 *(c) Translation*
455 Upon $HgCl_2$ exposure 83% and 74% of ribosomal proteins (r-proteins) were
456 down-regulated at 10 and 30 min, respectively, versus only 4% and 41% for PMA at the

457 corresponding times (Figures 5 and S9; data for all functional group heat maps are
458 shown in Table S13 and Table S14). Transcription of r-proteins is repressed directly by
459 binding of the nutritional stress-induced nucleotide ppGpp and DksA protein to RNAP
460 [48]. The ppGpp synthase genes, *spoT* and *relA*, were down-regulated or unchanged,
461 but expression of *dksA* was up-regulated for both $HgCl_2$ and PMA exposure. R-protein
462 expression can also be inhibited by excess r-proteins binding to and inhibiting
463 translation of their own mRNAs [49, 50].
464 Translation initiation and elongation factors were largely unchanged, but
465 expression of all three peptide chain release factor genes were down-regulated for PMA
466 and the ribosome recycling factor (*frr*) was up-regulated only for PMA, consistent with
467 interruption of translation. Eight tRNA-synthase genes declined with $HgCl_2$ but PMA
468 caused only four tRNA-synthase genes to decline and two to increase in expression
469 (Table S14). Both mercurials caused a relative decline in tRNA expression for most
470 amino acids, especially arginine, lysine, methionine, tyrosine, and valine tRNAs. With
471 very few exceptions, ribosome assembly and translation were shut down for up to 30
472 min by both compounds, but returned to normal levels by 60 min.
473
474 *(d) Macromolecular turnover and chaperones*
475 Divalent inorganic mercury can stably crosslink proteins and their subdomains
476 via cysteines, disrupting 3-dimensional structures and allosteric movements [51-53].
477 Although monovalent PMA cannot cross-link, it forms a bulky adduct with cysteines [23],
478 which may compromise protein folding. The proteases and chaperones of the heat
479 shock response degrade or repair misfolded proteins [54] and we found their expression

480 was increased by both mercurials (Figures 6 and S12 and Table S13). At 10 min,
481 expression of protease genes *lon, clpXP,* and *ftsH* had risen 4- to 6-fold with $HgCl_2$ and
482 *lon* and *clpXP,* but not *ftsH,* were up-regulated 3-fold with PMA. $HgCl_2$ provoked up-
483 regulation of all 12 heat shock protein (HSP) and chaperone genes by 10 min, but only
484 chaperones *clpB* and *ybbN* mRNAs remained elevated at 30 min. Two other HSP
485 genes, Hsp15 (*hslR*) involved in stalled ribosome recycling and Hsp31 (*hchA*) an amino
486 acid deglycase, were further up-regulated by $HgCl_2$ at 60 min. In contrast, at 10 min
487 PMA had up-regulated only five HSPs, increasing to six by 30 min and declining to three
488 by 60 min. The *ibpA* and *ibpB* chaperone genes were among the most highly up-
489 regulated genes for both $HgCl_2$ and PMA and persisted throughout recovery.
490 Of the 16 RNases and RNA processing enzymes only 3 increased: RNase R (3-
491 fold for $HgCl_2$ and 5-fold for PMA) for both compounds during first 30 min; RNase III
492 two-fold for PMA at 30 min; and RNase T two-fold for $HgCl_2$ at 60 min. The
493 degradasome complex subunit genes (*rne, eno, rhlB, pnp, ppk*) [55] were all down-
494 regulated for PMA during the first 30 min following exposure, except the helicase (*rhlB*),
495 but only enolase was down-regulated for $HgCl_2$ (Figures 6 and S12 and Table S13).
496 Expression of RNase II (*rnb)* was also down-regulated for both compounds, but with
497 relatively greater fold-changes observed for PMA. It is unclear what effect these
498 changes in gene expression could have on RNA turnover and message decay rates
499 while under mercury stress. As with the DNA metabolism genes, expression of the
500 transcriptional apparatus shows that sufficient PMA was taken up to elicit both positive
501 and negative responses distinct from $HgCl_2$.
502

503 ii. ENERGY PRODUCTION

504 *(a) Electron transport chain*

505 Expression of approximately 50% of all electron transport chain (ETC) genes was
506 down-regulated during the first 30 min for $HgCl_2$ and PMA, with individual gene
507 responses being very similar for both compounds (Figures 7 and S13 and Table S13).
508 By 60 min, only 26% of these genes were down-regulated for $HgCl_2$, and none were
509 down-regulated for PMA. Expression of NADH:unbiquinone oxidoreductase genes was
510 down-regulated by both compounds, with 77% and 100% of these genes being down-
511 regulated at 10 and 30 min, respectively. The ATP-synthase subunit genes were also
512 strongly down-regulated by both mercurials at 10 and 30 min, but normal expression
513 was restored at 60 min.

514 The *torCAD* locus that encodes the trimethylamine N-oxide anaerobic respiratory
515 system was strongly up-regulated only by PMA exposure. This is likely an artifact of
516 low-level basal expression and the dimethyl sulfoxide used to dissolve PMA. The final
517 DMSO concentration, 0.015% vol/vol (2.1 mM), was not expected to have any biological
518 effect [56] and the anaerobic DMSO reductase genes (*dmsABC*) were down-regulated.
519 It is unlikely that either the *tor* or *dms* responses affect growth rate [57] or afford
520 protection against either mercurial since over-expressed heme-dependent *torC* may be
521 in the apoprotein form [58].

522

523 *(b) Carbon metabolism*

524 Expression of genes for carbon metabolism decreased generally, but there were
525 more up-regulated genes in response to $HgCl_2$ and not all steps were affected equally

526 by both mercurials (Figure S14). Expression of five genes of the pentose-phosphate
527 pathway rose in at least one time point for $HgCl_2$, but only *pgl* increased for PMA at 10
528 min. The ribose-5-phosphate isomerase gene (*rpiB*), which is a backup enzyme for the
529 gene product of *rpiA* [59], was up-regulated 40-fold for $HgCl_2$ at 10 min; although
530 expression of *rpiA* did not differ from the unexposed cells for either mercurial at any
531 time. Glycolysis responded similarly to both mercurials, with the greatest number of
532 these genes being down-regulated at 30 min. The expression changes in TCA cycle
533 genes were distinct for $HgCl_2$ and PMA; six genes were up-regulated in at least one
534 time point for $HgCl_2$ and only one was up-regulated for PMA. Expression of several
535 carbohydrate transport genes was down-regulated by both mercurials (Table S6).
536
537 *(c) Nicotinamide adenine dinucleotide (NAD)*
538 Expression of genes for nicotinamide adenine dinucleotide (NAD) and NAD-
539 phosphate (NADP) synthesis and turnover pathways was repressed by mercury
540 exposure (Figure S15). The biosynthesis genes were moderately down-regulated, with
541 *nadB* being the only gene down-regulated for both mercurials at all times and *nadA*
542 decreasing for $HgCl_2$ at 30 and 60 min and for PMA at 30 min. Expression of the
543 *pncABC* salvage pathway did not change. The NAD reduction pathways were more
544 affected than the NADP reduction pathways, with only *pgi* down-regulated for both
545 mercurials and *edd* down-regulated only for $HgCl_2$. The transhydrogenase (*pntAB*) was
546 down-regulated only for PMA at 10 and 30 min. Expression of other genes for NAD to
547 NADH reduction in glycolysis and the TCA cycle were also down-regulated for both

548 mercurials, which reflects the overall decrease in metabolism and energy production
549 pathways.
550 Globally, redox metabolism declined immediately after exposure and normal
551 gene expression levels were not restored until growth recovered to the pre-exposure
552 rate. KEGG maps created using iPath [60] depict system-wide metabolism changes
553 over time (Figures S16-S18 for $HgCl_2$ and Figures S19-S21 for PMA).
554
555 iii. CENTRAL METABOLISM
556 *(a) Amino acid metabolism and transport*
557 The two mercurials had distinct effects on expression of genes for biosynthesis of
558 amino acids (Figure 8 and S22). Since mercury targets cysteine thiol groups and will
559 deplete the cellular reduced thiol pool, we expected an increase in cysteine and
560 glutathione biosynthesis. Surprisingly, most genes for biosynthesis of these biothiols
561 and for general sulfur metabolism were down-regulated or no different from the
562 unexposed cells, with the exception of up-regulation of *cysE*, which is the first step in
563 the biosynthesis pathway from serine.
564 Methionine biosynthesis gene expression increased for 7 genes with $HgCl_2$, but
565 11 genes were down-regulated with PMA, especially *metE* dropping 187-fold with PMA
566 at 30 min (Figure 8 and S22). Expression of genes for histidine synthesis also
567 responded differently to each mercurial, rising dramatically with $HgCl_2$ at 30 to 60 min.
568 In contrast, all *his* genes expression dropped with PMA from 10 to 30 min. Genes for
569 the synthesis of leucine, isoleucine, and valine had the opposite response, with most
570 down-regulated with $HgCl_2$ but up-regulated with PMA. Expression of other amino acid

571 biosynthetic pathways was largely unchanged or declined with both mercurials.
572 Branched-chain (*livKHMGF*), dipeptide (*dppABCDF*), and oligopeptide (*oppABCDF*)
573 transporters were also down-regulated for both mercurials, with greater relative negative
574 fold-changes for PMA (Table S5).
575
576 *(b) Inorganic ion transport and metallochaperones*
577 Inorganic Hg(II) can displace beneficial thiophilic metals from their native binding
578 sites in proteins, potentially affecting transport and disrupting transition metal
579 homeostasis [23], leading to expression changes for non-ferrous metal cation and
580 oxoanion transporters (Figures 9 and S23 and Table S13), iron homeostasis (Figures
581 10 and S24 and Table S13) and metal-binding proteins and enzymes (Table S15).
582 Inorganic mercury exposure releases labile iron, which could itself increase
583 oxidative stress via Fenton chemistry under aerobic growth [23, 61]. Most iron uptake
584 pathways declined early for both mercurials, consistent with the observed increase in
585 expression of the Fur repressor. The cytochrome *c* maturation genes that transport
586 heme to the periplasm (*ccmABCDE*) were also down-regulated for both mercurials. The
587 putative ferrous iron and zinc efflux pump, *fieF* [62] increased 2-fold for $HgCl_2$ at 10 min
588 only, suggesting it may have a transient role in restoring one or both of these
589 homeostases.
590 There are two iron-sulfur (Fe-S) cluster assembly pathways in *E. coli* [63, 64].
591 Expression of the primary Isc system (*iscRSUA*, *hscBA*, and *fdx*) increased strongly for
592 both mercurials, but with greater relative changes for $HgCl_2$ (Figures 10 and S24 and
593 Table S13). The secondary Fe-S cluster assembly system *sufABCDSE*, which activates

594 under oxidative stress or iron limiting conditions also increased greatly, but only for
595 $HgCl_2$. These transcriptional responses confirm and extend biochemical findings [23]
596 that Fe-S clusters are more vulnerable to inorganic mercury than to organomercurials
597 and the cell quickly tries to repair this damage.

598 Expression of the zinc transporter *zupT* increased modestly in the 3- to 5-fold
599 range for both mercurials during the first 30 minutes (Figures 9 and S23 and Table
600 S13). In contrast, expression of the P-type ATPase zinc efflux pump, *zntA* [65]
601 increased in the 20- to 40-fold range for both mercurials at 10 and 30 min and the
602 periplasmic Zn-binding protein ZraP was up-regulated throughout recovery. *E. coli* has
603 two copper/silver efflux systems, Cue and Cus [66]. Surprisingly, the Cus system genes
604 (*cusRS, cusCFBA)* primarily used under anaerobic conditions were among the most
605 down-regulated genes under PMA exposure. The Cue system consists of the multi-
606 copper oxidase, CueO, and a P-type ATPase, CopA, both regulated by the MerR
607 homolog, CueR. Genes *cueO* and *copA* were up-regulated approximately 20-fold with
608 $HgCl_2$ at both 10 and 30 min whereas they increased 5-fold with PMA only at 10 min.
609 The nickel uptake system [67] (*nikABCDER*) was also strongly down-regulated under
610 PMA exposure conditions through all times although expression of repressor NikR was
611 unchanged, except for a 3-fold increase with $HgCl_2$ at 10 min. Expression of the nickel
612 and cobalt efflux gene, *rcnA*, increased with $HgCl_2$ or PMA. Manganese (*mntH*), and
613 magnesium (*mgtA, corA*) uptake genes increased with both mercurials.

614 Inorganic anions used by *E. coli* include phosphate, sulfate, and molybdate and
615 the genome also encodes genes for defense against arsenate, which acts as a
616 phosphate mimic (Figures 9 and S23 and Table S13). Expression of the ABC

617 phosphate transport system (*pstSCAB*) genes increased greatly for both mercurials,
618 with PMA-provoked changes up to 165-fold, relative to unexposed condition, for the
619 phosphate binding protein, *pstS*. The two-component phosphate regulatory system,
620 PhoBR, was up-regulated for both mercurials; *phoB* changed up to 22-fold with $HgCl_2$
621 and 105-fold with PMA relative to the unexposed condition. Sulfate and thiosulfate
622 uptake by the ABC transporter (*cysPUWA*) decreased strongly with $HgCl_2$ at 30 min and
623 PMA at 10 and 30 min. Expression of molybdate uptake (*modABC*) increased with PMA
624 during the first 30 min but only at 10 min with $HgCl_2$. The arsenate resistance operon
625 cannot effect Hg(II) resistance, but was highly induced by both mercurials, perhaps
626 through interacting with the three-cysteine metal-binding site of the ArsR repressor [68].
627
628 iv. SURFACE FUNCTIONS
629 *(a) Cell wall biogenesis, porins, lps, efflux systems, and electrolyte balance*
630 The transcriptional response of peptidoglycan, membrane biosynthesis, and cell
631 division genes was similar for both mercurials (Figure S25 and Table S13). Expression
632 increased for roughly 20% of lipid biosynthesis genes, including those for cardiolipin,
633 and expression decreased for 20-30% of other lipid-related genes. Transcription of
634 genes for murein synthesis (*murCDEFGIJ*) in particular declined for both mercurials
635 during the first 30 min.
636 *E. coli* encodes several antibiotic resistance efflux systems that are up-regulated
637 by mercury exposure (Figures 11 and S26 and Table S13). The multiple antibiotic
638 resistance locus (*marRAB*), which increases drug efflux and also limits passive uptake
639 by decreasing porin expression [69], was strongly up-regulated by both mercurials with

640 greater fold-changes observed for PMA, relative to the unexposed condition. Though
641 expression of some porin genes (*ompC, ompF, ompT, ompW*) was repressed, three
642 non-specific porins (*ompG, ompL, ompN*) were up-regulated only by PMA. Genes from
643 several TolC-dependent antibiotic efflux systems were up-regulated by both mercurials
644 as well, including *acrEF, emrD, emrKY,* and several *mdt* genes [70]. $HgCl_2$ exposure
645 alone also up-regulated two-component sensor genes (*phoQP* at 10 min and *basSR* at
646 60 min) that regulate genes involved in modification of the cell surface and increase
647 polymyxin resistance [71], but most of these genes were down-regulated or unchanged
648 for PMA.

649 The response to osmotic stress and maintenance of electrolyte balance are
650 important membrane functions requiring adaptation in dynamic natural environments.
651 During $HgCl_2$ exposure the expression of the sodium antiporter, NhaA, increased 4-fold
652 at 10 min and the calcium/potassium antiporter, ChaA, was up-regulated 3-fold at 10
653 and 30 min (Figures 9 and S23 and Table S13). In contrast, expression of genes for
654 transport of the major electrolyte, potassium, changed only modestly in some subunits
655 of the *kdp, kef*, and *trk* systems, without an obvious response pattern. However,
656 transcription of genes for defense against osmotic stress was uniformly up-regulated;
657 betaine genes (*betABIT and proP*), *osmBCEFY, and* mechanosensitive channel
658 proteins (*mscL* and *mscS*) increased for both mercurials, as did a putative
659 osmoprotectant ABC permease (yehYXW) [72] only with $HgCl_2$ at 30 and 60 min (Table
660 S5).

661

662 *(b) Motility and biofilm*

663 Nearly all flagellar component genes were strongly down-regulated for both
664 mercurials, with greater negative fold-changes observed with PMA relative to the
665 unexposed condition (Figures 12 and S27). Only PMA increased expression of fimbriae
666 and curli fiber genes, which alter motility and increase adhesion (Figure 13 and S28)
667 [73]. Fifteen genes up-regulated by PMA exposure were annotated as homologs of
668 FimA, but with unknown function. FimA is the major structural component of fimbriae,
669 but these genes may serve other functions. Motility genes whose expression dropped
670 remained low until 60 min with $HgCl_2$, indicating that the structurally and energetically
671 intensive motility systems are very slow to recover.
672 $HgCl_2$ and PMA also provoked expression of several biofilm-related genes
673 (Figures 13 and S28 and Table S13). The *bhsA* and *bdcA* loci were among the most
674 highly up-regulated genes during $HgCl_2$ exposure, with a relatively greater fold-change
675 than observed for PMA (Tables 2 and 3). Neither gene is well characterized, but
676 independently each has been found to decrease biofilm formation and increase
677 resistance to external stressors [74, 75]. Only PMA increased expression of genes for
678 poly-β-1,6-N-acetyl-glucosamine (PGA) polysaccharide production [76] and biofilm
679 related genes, *ycgZ, ymgA, ariA, ymgC* [77]. Thus, PMA elicits a broader response that
680 potentially alters the cell surface and may increase adhesion and biofilm formation; in
681 contrast $HgCl_2$ only inhibits motility and does not activate adhesion pathways. It is
682 possible that some changes observed for motility and biofilm related genes following
683 PMA-exposure are an artifact of the DMSO, but other studies suggest that solvent
684 would have no effect or that much higher concentrations than used here would be
685 required to induce these changes [56, 78].

686

687 v. STRESS RESPONSES

688 *(a) Oxidative stress response and repair*

689 There are two oxidative stress response pathways in *E. coli*, the *oxyRS* and
690 *soxRS* regulons [61, 79]. OxyR, a LysR-family transcriptional regulator, uses a cysteine-
691 pair to sense oxidative damage and regulates 49 genes when oxidized [80]. $HgCl_2$
692 exposure increased expression of 22 OxyR regulon genes at 10 min; these then
693 declined to 13 genes by 60 min (Table S16). In contrast, PMA provoked expression of
694 16 OxyR regulon genes at 10 and 30 min, but none at 60 min. *OxyS*, a small non-
695 coding RNA regulated by OxyR, represses *rpoS*, *fhlACD* and other genes to prevent
696 redundant induction of stress response genes [81]. The *oxyS* gene was among the most
697 highly differentially expressed genes, increasing over 1,000-fold with $HgCl_2$ at 10 and 30
698 min relative to the unexposed condition. Differential expression of *oxyS* was more
699 modest with PMA having a relative increase of 10-fold at 10 min and 6-fold at 30 min.

700 The SoxRS regulon is the other oxidative stress response system in *E. coli*.
701 SoxR, a MerR-family repressor-activator, uses the oxidation state of 2Fe-2S clusters to
702 respond to superoxide (O_2^-) stress and induce transcription of *SoxS* [82-85], which then
703 transcriptionally regulates 53 genes [79, 86] (Table S16). $HgCl_2$ or PMA exposure up-
704 regulated 22 or 25 genes, respectively, at 10 min and these had declined to 13 or 0
705 genes, respectively by 60 min.

706 Key genes in these oxidative stress regulons differentially expressed upon
707 mercury exposure include the ROS scavengers: catalase (*katG*), alkyl hydroperoxide
708 reductase (*ahpCF*), and superoxide dismutase (*sodA*) (Figures 14 and S29 and Table

709 S13). Thiol homeostasis genes included *gor*, *grxA,* and *trxC* (Figures 14 and S29 and
710 Table S13). Iron homeostasis and the Fe-S cluster assembly and repair genes (*fur, dps,*
711 *fldA, fpr, hemH, sufABCDES,* and *yggX*) were also up-regulated. PMA provoked
712 comparatively lower fold-changes than $HgCl_2$ for *grxA, trxC, ahpC, dps, fldA, hemH, and*
713 *yggx*. The manganese uptake protein, *mntH*, plays an important role in ROS resistance
714 [87] and was up-regulated for both mercurials. Oxidation-resistant dehydratase
715 isozymes, *acnA* and *fumC* [88, 89] also increased, but only for $HgCl_2$ exposure. Thus,
716 both mercurials triggered the Oxy and Sox oxidative stress responses, but $HgCl_2$
717 elicited greater fold-changes overall than PMA compared to unexposed cells.
718 Because mercury poisons the cellular thiol pool [23], we expected that regulation
719 of redox homeostasis proteins such as glutaredoxins, thioredoxins and glutathione-
720 related genes would respond to mercury exposure (Figure 14 and S29). Glutaredoxin 1
721 (*grxA*) expression was up-regulated for both mercurials, with a greater fold-change
722 observed for $HgCl_2$ relative to unexposed condition. In contrast, glutaredoxin 2 (*grxB*)
723 was down-regulated for both mercurials, while glutaredoxin 3 (*grxC*) and glutaredoxin 4
724 (*grxD*) were up-regulated only for PMA. Thioredoxin reductase (*trxB*) was up-regulated
725 2-fold with PMA only at 30 min, but was up-regulated with $HgCl_2$ 8-fold (10 min) and 4-
726 fold (30 min). Thioredoxin 1 (*trxA*) expression increased 2-fold only with PMA (10 min);
727 in contrast to thioredoxin 2 (*trxC*), which was up-regulated for both mercurials, but had
728 greater fold-change relative to the unexposed condition with $HgCl_2$ than with PMA.
729 However, the thiol peroxidase (*tpx*) was up-regulated modestly for PMA, but did not
730 change for $HgCl_2$. Thus, while each mercurial stresses the cell to maintain redox
731 homeostasis, $HgCl_2$ exposure elicited greater responses.

732 Glutathione (GSH) serves as the cell's redox buffer and as a scavenger of
733 mercurials (Figures 14 and S29 and Table S13). Surprisingly, expression of GSH
734 biosynthesis and utilization genes increased only modestly. The
735 γ-glutamyltranspeptidase (*ggt*) increased late (60 min) by 4-fold only with $HgCl_2$. GSH
736 synthase (*gshA*) did not change and *gshB* was up-regulated 2- or 3-fold for both
737 mercurials only at 10 min. The GSH importer (*gsiABCD*) may be a salvage pathway to
738 recover GSH and cysteine leaked into the periplasm by CydCD [90, 91], but it was
739 down-regulated by $HgCl_2$ or PMA through 30 min. The GSH reductase (*gor*) increased
740 only with $HgCl_2$ at 10 min and several GSH S-transferase genes involved in
741 detoxification [92] (*gstA, gstB, yfcF, yqjG, yibF, yncG*) increased with both mercurials.
742 Since all of these proteins have Hg(II)-vulnerable cysteines in their active sites, it is
743 surprising that neither Hg(II) nor PMA-challenged cells provoked increased expression
744 and suggests that their normal mRNA levels are sufficient to replenish them.
745
746 *(b) Genes with delayed up-regulation*
747 Genes unchanged at 10 min but differentially expressed at both 30 and 60 min or
748 60 min alone may be those needed as cells transition out of stasis and towards normal
749 growth (Table S17). For $HgCl_2$ exposure, 95 genes were up-regulated and 140 genes
750 were down-regulated that display this delayed response pattern. Approximately half of
751 the up-regulated genes are involved in energy production, transport and metabolism
752 pathways based on COG annotations. Roughly 45% of these delayed $HgCl_2$ provoked,
753 up-regulated genes are the same as genes that were differentially expressed during the
754 first 30 min of PMA exposure. This overlap is consistent with slower recovery of growth

755 in $HgCl_2$ exposed cells and that some of the same pathways are used for recovery by
756 both compounds. In contrast, for the more quickly recovering PMA exposure, of the
757 genes that showed no change at 10 min only six were up-regulated at 60 min (Table
758 S17). Only two of these delayed-response genes for PMA exposure overlapped with up-
759 regulated genes for $HgCl_2$ exposure.
760

761 **DISCUSSION**

762 Mercury is a ubiquitous toxicant that serves no biologically beneficial role.
763 Exposure to any form of mercury negatively impacts the health of organisms from
764 microbes to humans. The biological effects of different forms of mercury are often
765 conflated and methylmercury is assumed to be the most toxic form. However, the
766 systemic biochemical and molecular differences between inorganic and organic mercury
767 compounds have yet to be well characterized from exposure through recovery in a
768 single model system.
769

770 ***BULK DIFFERENTIAL EFFECTS ON GROWTH AND GENE EXPRESSION***

771 The sub-acute mercury exposure conditions used in this study were chosen by
772 identifying a mercury concentration high enough to stop cells from doubling, but low
773 enough to allow restoration of the pre-exposure growth rate within one-hour (~1
774 generation period) after exposure (Figure 1a). Concentrations below 3 μM of either
775 compound did not consistently inhibit growth and higher concentrations of $HgCl_2$ did not
776 allow recovery within the desired time frame. The 3 μM Hg used in this study is well
777 within the range that bacteria can experience chronically from dental amalgam fillings

778 [93] and in highly contaminated environments, such as artisanal gold mining operations
779 [8]. Mercury in tuna is 0.386 ppm compared to the proxy organomercurial, PMA, used
780 here at 3 μM or 0.6 ppm [94].

781 PMA-exposed cells recovered exponential growth faster (Figure 1) than those
782 with equimolar exposure to $HgCl_2$, perhaps owing to lower uptake of PMA (Table S2).
783 However, PMA-exposed cells differentially expressed more genes than $HgCl_2$ exposed
784 cells during the first 30 min of exposure (Figure 1b). These results agree with
785 observations in *C. elegans,* where MeHg exposure resulted in four times more DEGs
786 than did $HgCl_2$ for all concentrations tested [95]. However, in contrast to *E. coli,* whose
787 growth was inhibited more by inorganic $HgCl_2$, in *C. elegans* the effective toxic
788 concentration of methylmercuric chloride was lower than for $HgCl_2$ [95]. The large
789 number of significant DEGs in response to mercury exposure is greater than the
790 response to hydrogen-peroxide [96] or nitric-oxide [97], but other types of chemical
791 exposures to organic acids [98] and volatile organic compounds [99] in *E. coli* have
792 resulted in similar numbers of DEGs to mercury exposure and the stress response
793 sigma factor RpoS has been shown to regulate up to 23% of the genome alone [100].

794 We found that most DEGs peaked at 10 min after exposure for both compounds
795 with $HgCl_2$ provoking more down-regulated genes and PMA yielding more up-regulated
796 genes throughout the exposure period (Figure 1b). Even though the optical density (OD)
797 of the $HgCl_2$ exposed culture showed no growth recovery from 10 min to 30 min, DEGs
798 decreased by 22%, while PMA-exposed cells over the same period had a moderate
799 increase in OD, but only an 8% decrease in DEGs (Figure 1). In contrast in a eukaryotic
800 system, the livers of $HgCl_2$ exposed zebrafish continuously increased in DEGs

801 throughout the observed 96 hour exposure period as mercury accumulated in their cells
802 [101].
803 In *E. coli,* during the first 30 min post-exposure, 50-70% of both up- and down-
804 regulated genes were the same for both compounds (Figure 2), but at the level of
805 individual genes there were both qualitative and quantitative differences in expression
806 (Table S5), consistent with idiosyncratic transcriptional responses to each compound.
807 The nematode *C. elegans* also manifested distinct and even some opposite
808 transcriptional responses to inorganic and organic mercury exposure in a single end-
809 point microarray experiment [24].
810 As there are not yet other studies of the global transcriptional response of a
811 bacterium to mercury exposure, on the basis of the findings in eukaryotes and our
812 proteomic work [23] we have organized our observations here into those we had
813 expected and those we did not expect from any yet published work.
814
815 ***EXPECTED AND UNEXPECTED GENE-SPECIFIC CHANGES***
816 *Expected transcriptional changes:*
817 *(a)* Thiol homeostasis. The millimolar cytosolic pool of glutathione (GSH) can sequester
818 mercurials and thereby protect protein thiols from binding strongly to these soft metal
819 toxicants. However, if the GSH pool becomes depleted by mercury complexation, the
820 cell loses this primary defense mechanism. Since proteins of the stress response and
821 repair pathways all contain active site thiols, often as part of Hg(II)-vulnerable Fe-S
822 centers, it is not obvious how a cell that has lost much of its available thiols to Hg(II)
823 chelation can restore its metabolism. Given this, we expected cysteine and glutathione

824 biosynthesis pathways to be up-regulated. However, cysteine biosynthesis was down-
825 regulated (Figures 8 and S22 and Table S13) and GSH biosynthesis was mostly
826 unchanged (Figures 14 and S29 and Table S13) for both compounds, in contrast to the
827 eukaryotic response to mercury [101-103] and H_2O_2 exposure [96], which increase GSH
828 and metallothionein production. However, although thiol biosynthesis did not increase,
829 genes involved in maintaining cellular thiol homeostasis did increase (Figures 14 and
830 S29 and Table S13); thioredoxin (*trxC*) and glutaredoxin (*grxA*) were among the most
831 highly up-regulated genes with $HgCl_2$ and PMA exposure. Others have also found in *E.*
832 *coli* that glutathione reductase increased with $HgCl_2$ and both compounds increased
833 expression of glutathione oxidoreductase and S-transferase genes, which protect
834 against oxidative stress and xenobiotics [104].
835
836 *(b)* Iron homeostasis. We also expected inorganic mercury to disrupt iron-sulfur clusters
837 with consequent effects on Fe homeostasis generally [23, 105]. Iron uptake was down-
838 regulated with both mercurials, consistent with excess intracellular free Fe(II) and
839 general oxidative stress, but expression of the uptake repressor (*fur*) was only up-
840 regulated for $HgCl_2$ (Figure 10 and S24). *Fur* expression is activated by either OxyR or
841 SoxS [96, 106] and Fur represses Fe uptake pathways with ferrous iron as a co-
842 repressor [107]. Fur can also bind other divalent metals [108], so Hg(II)-Fur might mimic
843 Fe-Fur as an iron uptake repressor under these conditions to limit Fenton-mediated
844 damage from excess iron. Although both mercurials increased expression of the primary
845 Fe-S cluster assembly and repair system (*isc*), only $HgCl_2$ induced the secondary
846 system (*suf*), which is normally induced under oxidative stress or iron limiting conditions

847 [63, 109] (Figures 10 and S24 and Table S13). Also, only $HgCl_2$ exposure increased
848 expression of iron storage proteins: ferritin, bacterioferritin, and Dps (Figure 10 and
849 S24). The DNA binding protein Dps which binds free iron to protect DNA from ROS
850 damage [110] was one of the most highly up-regulated genes with $HgCl_2$ exposure
851 (Table 1).
852
853 *(c)* Oxidative stress response. The known close link between iron homeostasis and
854 oxidative stress [61] explains the large fold-changes observed upon $HgCl_2$ exposure in
855 genes that respond to oxidative stress (Table S16) and echoes mercury's long known
856 stimulation of oxidative damage in rat kidney mitochondria [111]. The small non-coding
857 RNA *oxyS* was the second most highly up-regulated gene upon $HgCl_2$ exposure with
858 differential expression more than 100-fold greater than observed for PMA (Table 1). The
859 ROS scavenger *ahpF* was also highly up-regulated, along with *katG* (early) and *sodA*
860 (delayed) but only for $HgCl_2$ (Figures 14 and S29 and Table S16). Other ROS resistant
861 enzymes, aconitase A [89] and fumarase C [112] (Table S16) also increased only for
862 $HgCl_2$, as did the manganese-dependent alternative ribonucleotide reductase genes
863 (*nrdHIEF*) [113]. The glutaredoxin-like protein that functions like thioredoxin, *nrdH* [114],
864 was highly up-regulated by $HgCl_2$ and might support other thioredoxin and glutaredoxin
865 proteins. These striking differences in gene expression illuminate how *E. coli* modulates
866 expression of specific genes not only to deal with compromised function of specific
867 $HgCl_2$ modified proteins, but also to manage the consequent cascade of reactive oxygen
868 species.
869

870 *(d)* Heat shock response. Mercurials bound to protein cysteines could disrupt protein
871 folding, subunit assembly, and allosteric movements [52, 115] and inorganic mercury
872 can crosslink neighboring cysteines leading to aggregation [51]. Increased expression
873 of heat shock response genes was expected as a consequence of such anticipated
874 protein misfolding problems [116]. Indeed, expression of heat shock chaperonins and
875 protease genes increased for both mercurials, with more genes up-regulated early in
876 response to $HgCl_2$ than to PMA (Figures 6 and S12 and Table S13). Genes for the
877 small chaperone-like proteins, *ibpA* and *ibpB*, were among the most highly increased for
878 both compounds, especially for $HgCl_2$ (Table 1), consistent with their role in aiding Lon
879 protease in the degradation of misfolded proteins [117-119].
880
881 *(e)* Translational apparatus. Thiophilic Cd^{2+} exposure in *E. coli* has been shown to
882 decrease expression of ribosomal proteins [120]. In our proteomics work (Zink et al. in
883 preparation) we observed fourteen r-proteins (7 for each ribosomal subunit) that formed
884 stable adducts with either PMA or Hg(II), so it was reasonable to expect this to be
885 reflected in transcription of r-proteins. Indeed, $HgCl_2$ exposure repressed expression of
886 up to 83% of r-protein genes at 10 min and 74% at 30 min (Figure 5, S11, and Table
887 S14), whereas PMA only transiently repressed expression of 41% of r-proteins at 30
888 min. Divalent inorganic mercury's ability to cross-link proteins may interfere with
889 ribosome assembly resulting in translational feedback and repression of r-proteins
890 transcription. Disruption of ribosome assembly could also contribute to the slower
891 recovery of growth after inorganic Hg(II) exposure.
892

893 *(f)* Energy production. The dependence of most energy production pathways on redox-
894 active transition metals and redox-active sulfur compounds made them obvious targets
895 of mercurial disruption, e.g. three ATP-synthase subunits form stable adducts after in
896 vivo exposure to Hg(II) or PMA (Zink et al. in preparation). Expression of genes within
897 this functional category was largely down-regulated early in exposure, with all nine
898 ATPase subunits down-regulated for $HgCl_2$ (10 min) and eight down-regulated for PMA
899 (30 min) (Figure 7 and S13). Although others have found that Cd exposure in *E. coli*
900 repressed aerobic energy metabolism genes and induced anaerobic pathways [120], we
901 found that both aerobic and anaerobic energy metabolism were repressed by $HgCl_2$ and
902 PMA. Even though expression of the oxygen-sensing *fnr* [121] and *aer* [122, 123]
903 activators of the anaerobic shift were moderately up-regulated for PMA and unchanged
904 for $HgCl_2$ (Table S5). Similarly, glucose metabolism genes were also predominantly
905 down-regulated during early periods for both compounds, especially with PMA exposure
906 (Figure S14). Thus, with severely compromised energy production systems, it is not
907 surprising that amino acid, carbohydrate and nucleotide metabolism genes, and the
908 energy-dependent transport of these molecules (Figure 3 and Table S6), are also
909 largely depressed initially.
910
911 *(g)* Homeostases of non-ferrous metals. We expected mercurials to disrupt electrolyte
912 balance [23], but expression of the potassium efflux pumps' subunit genes (*kcpABC,*
913 *kefBC, and trkAGH*) were not uniformly up-regulated, although the need to restore the
914 pH balance was indicated by transiently increased expression of the H^+/Na^+ antiporter
915 (*nhaA*) for both compounds (Figures 9, S23 and Table S5). It may be that normal levels

916 of the proteins involved in maintaining cellular electrolyte balance are sufficient to
917 respond to mercury exposure and a significant change in transcriptional expression is
918 not required for these genes.

919 Mercury is also expected to disrupt non-ferrous metal homeostasis because it
920 can displace other metals, such as zinc and copper, as enzyme cofactors [124, 125].
921 Expression of metal uptake genes decreased and of metal efflux genes increased for
922 zinc, copper, nickel and cobalt, with relatively greater fold-changes occurring with $HgCl_2$.
923 Zinc efflux by ZntA is regulated by the MerR homolog ZntR, which can respond to Hg(II)
924 [126], but has not been shown to confer resistance to Hg(II) exposure. Up-regulated
925 periplasmic transition metal binding proteins, ZraP [127] and ZinT [128], use histidine
926 residues to coordinate metal binding and all cysteine residues present in either protein
927 are involved in structural disulfide bonds that prohibit availability for binding metals.
928 Thus, these periplasmic metal binding proteins lack requisite thiol ligands [23] to
929 compete for Hg effectively with periplasmic glutathione [90, 129, 130]. Their increased
930 transcription here likely reflects their control by a complex suite of redox and other
931 stress regulators [86] provoked by Hg exposure as reported above. Manganese may
932 protect iron metalloenzymes under oxidative stress conditions [87] and Mn uptake by
933 *mntH,* as part of the OxyR regulon, was correspondingly up-regulated for both
934 compounds in response to mercury-induced oxidative stress.
935

936 *Unexpected transcriptional changes:*

937 *(a)* Motility and chemotaxis. Energetically costly flagellar motility and chemotaxis were
938 strongly down-regulated by both mercurials and were among the slowest to recover

939 normal transcription levels (Figures 12 and S27 and Table S13). Motility gene
940 expression is regulated by σ^{28} (*fliA*) and FlhDC [131] and the expression of these two
941 regulatory genes declined with $HgCl_2$ but was unchanged with PMA. Repression of
942 motility may occur through sigma factor competition for binding to RNAP between σ^{28}
943 and increased expression of σ^{S} [132] and/or through repression of the flagellar
944 transcriptional activator FlhDC by increased expression of the small ncRNAs *oxyS* and
945 *gadY* [133]. Interestingly, $HgCl_2$ exposure impaired locomotion in *C. elegans* [24],
946 although through a very different mechanism of motility from *E. coli*.
947
948 *(b)* Surface appendages and biofilm synthesis. Surprisingly, there were large increases
949 in expression of genes involved in biofilm formation and adhesion or dispersal (Figures
950 13 and S28 and Tables S13). Expression of *bhsA* and *bdcA,* which function in biofilm
951 dispersal or reduced biofilm formation [74, 75], were the first and third, respectively,
952 most up-regulated genes by $HgCl_2$ (Table 1) and were also up-regulated for PMA, but
953 with relatively smaller fold-changes (Table 2). Expression of *bhsA* is also up-regulated
954 by other diverse stressors and may decrease cell permeability [75, 134]. PMA exposure
955 especially increased expression of genes for the polysaccharide PGA, which aids in
956 adhesion in biofilm formation [76], and other biofilm formation (*ycgZ, ymgA, ariA, ymgC*
957) genes [77] (Figures 13 and S28 and Table S13).
958 Expression of fimbriae (*fim)* and curli fibers (*csg*), important for adhesion in
959 biofilm formation [73] were also up-regulated only by PMA (Figure 13 and S28), as were
960 15 of 22 FimA homologs of unknown function. Outer membrane vesicle formation
961 (OMVs) could also play a role in detoxification, since an increase in formation of these

962 vesicles has been associated with heat shock, oxidative stress response, and biofilm
963 formation [135], which are responses up-regulated to varying degrees by both
964 mercurials. These are distinct differences between PMA and $HgCl_2$ response. PMA
965 provocation of biofilm formation and adhesion genes might be an artifact of its DMSO
966 solvent, but it is not obvious why $HgCl_2$ induces such high increases in biofilm dispersal
967 genes.
968
969 *(c)* Phosphate metabolism. Phosphate uptake genes were among the most highly up-
970 regulated genes for PMA exposure (Figure 9, S23, and Table 2). The PhoBR two-
971 component system controls expression of phosphate transport genes, as well as some
972 genes that increase virulence including those for fimbriae and biofilm formation [136].
973 Since expression of PhoBR and its regulon increases under phosphate limiting
974 conditions [137], it may be that PMA inhibits phosphate uptake by an unknown
975 mechanism, possibly through direct interaction with highly up-regulated PstS or this
976 could be an artifact of DMSO.
977
978 *(d)* Amino acid biosynthesis. Expression of most amino acid pathways was down-
979 regulated by both compounds, but a few responded uniquely to each mercurial (Figures
980 8 and S22 and Table S13). Since methionine auxotrophy occurs under oxidative stress
981 due to ROS susceptibility of methionine synthase (MetE) [138], expression of
982 methionine biosynthesis genes may have increased with $HgCl_2$ due to a stronger
983 oxidative stress response than PMA. However, since PMA did up-regulate some
984 oxidative stress-related genes, it is curious that Met operon expression was down-

985 regulated under PMA exposure. Next to its affinity for cysteine sulfur, Hg(II) binds the
986 imino nitrogen of histidine very strongly [139], so it was intriguing that histidine
987 biosynthesis genes were also up-regulated by $HgCl_2$ but down-regulated by PMA. It
988 remains unclear how these differences or the opposite responses for leucine, isoleucine
989 and valine biosynthesis help the cell survive mercurial exposure.
990
991 *(e)* Miscellaneous genes. Multiple antibiotic efflux systems and polymyxin resistance
992 surface modifications were up-regulated by $HgCl_2$ exposure, and even more so by PMA
993 (Figures 11 and S26 and Table S13). Chronic mercury exposure contributes to the
994 spread of multiple antibiotic resistant bacteria through co-selection of plasmid-borne
995 antibiotic and mercury resistance genes [140, 141]. Increased expression of antibiotic
996 resistance and surface components hint that low-level mercury exposure could prime
997 cells for increased antibiotic resistance. However, the ubiquity of plasmid- and
998 transposon-borne Hg resistance loci suggests that expression of these chromosomal
999 genes offers insufficient protection against the antibiotic or mercurial levels encountered
1000 in clinical practice.
1001 A handful of vestigial e14 or CPS-53 prophage genes were up-regulated by
1002 $HgCl_2$ (Table 1) or PMA (Table S5), respectively. Some are known to increase
1003 resistance to osmotic, oxidative, and acid stressors [142, 143], but their roles and
1004 mechanisms have not been well defined.
1005
1006 *(f)* Differential expression of genes required for the same functional protein complex.

1007 In many instances we observed that transcripts for subunits of the same enzyme,
1008 protein complex, or component of a tightly articulated pathway were differentially
1009 expressed. In some cases these proteins lie in distinct transcripts, which may
1010 experience different turnover rates and in other cases the differences could be due to
1011 transcriptional polarity. We have chosen not to deal explicitly with such paradoxes in
1012 this work, which is sufficiently complex as it is, but will address them in future work.
1013

1014 **CONCLUSIONS**

1015 The effects of mercury exposure in multicellular organisms have long been
1016 studied at the physiological level but a global, fine grained understanding of the
1017 differences in the precise biochemical sequelae of inorganic and organic mercury
1018 exposure has been lacking. This study is the first to examine not only the global
1019 transcriptional response differences between inorganic mercury ($HgCl_2$) and an
1020 organomercurial (phenylmercuric acetate) in a model microorganism, but also first to
1021 examine longitudinally how the cell recovers from these chemically distinct compounds.
1022 Taken together with global identification of vulnerable protein targets (Zink et al. in
1023 preparation) and of damage to thiol and metal ion homeostasis upon acute mercurial
1024 exposure [23], the current work provides a quantitative systems-level description of the
1025 effects of *in vivo* mercury exposure in *E. coli*. What was striking and most challenging
1026 with this study was the breadth and diversity of the systems whose expression was
1027 affected by these two chemically distinct mercurials. Sub-acute exposure influenced
1028 expression of ~45% of all genes with many distinct responses for each compound,
1029 reflecting differential biochemical damage by each mercurial and the corresponding

1030 resources available for repair. Energy production, intermediary metabolism and most
1031 uptake pathways were initially down-regulated by both mercurials, but nearly all stress
1032 response systems were up-regulated early by at least one compound. These results
1033 echo the wide functional variety of proteins stably modified by these mercurials owing to
1034 the widespread occurrence of cysteines found in nearly all *E. coli* proteins. Microbiome
1035 studies are rapidly unveiling the importance of commensal bacteria to the health of all
1036 higher organisms. Our findings in this model commensal organism provide insights into
1037 how chronic mercury exposure might affect such complex microbial communities and,
1038 consequently, the health of the host. This work also serves as a foundation for studies
1039 now underway of how the widely found mobile Hg resistance (*mer*) locus assists the cell
1040 in recovery from Hg exposure.
1041
1042 **LIST OF ABBREVIATIONS:**
1043 Hg = mercury
1044 $HgCl_2$ = mercuric chloride
1045 PMA = phenylmercuric acetate
1046 PhHg = phenylmercury
1047 DMSO = dimethyl sulfoxide
1048 LB = Luria-Bertani medium
1049 NM3 = Neidhardt MOPS minimal medium
1050 NGS = next generation sequencing
1051 DEGs = differentially expressed genes
1052 CVAA = cold vapor atomic absorption

1053 GSH = glutathione

1054 Cys = cysteine

1055 MDR = multidrug resistance

1056 ncRNA = non-coding RNA

1057 COGs = clusters of orthologous groups

1058 GOFs = gene-ontology functions

1059 RNAP = RNA polymerase

1060 HSP = heat shock protein

1061 ETC = electron transport chain

1062 PGA = poly-β-1,6-N-acetyl-glucosamine

1063

1064 **DECLARATIONS**

1065 **Ethics approval and consent to participate:** Not applicable

1066 **Consent for publication:** Not applicable

1067 **Availability of data and materials:** The tabulated datasets supporting the conclusions

1068 of this article are included as additional files. The read counts and raw sequence data

1069 (.fastq) are stored and available to the public through the Gene Expression Omnibus

1070 database (http://www.ncbi.nlm.nih.gov/geo/) with accession ID: GSE95575.

1071 **Competing interest:** The authors declare that they have no competing interests.

1072 **Funding:** US Department of Energy awards ER64408 and ER65286 to AOS

1073 **Authors' contributions:** SL conceived and designed experiments, prepared biological

1074 samples, extracted ribosomal depleted RNA for RNA-Seq, performed all data analysis,

1075 and drafted manuscript. AOS was a major contributor in experimental design, feedback

on data analysis, and in editing the manuscript. All authors read and approved the manuscript.

ACKNOWLEDGMENTS

We thank Roger Nilsen at the Georgia Genomics Facility for library preparation and Sharron Crane at Rutgers University for Hg content analysis. We also thank Bryndan Durham, Brandon Satinsky, Mary Ann Moran, Michael K. Johnson, Harry Dailey, Timothy Hoover, Anna Karls, Alexander Johs, Jerry Parks, Susan Miller, and Andrew Wiggins who have provided feedback and discussion on this work. This work was supported by US Department of Energy awards ER64408 and ER65286 to AOS.

REFERENCES

1. Driscoll CT, Mason RP, Chan HM, Jacob DJ, Pirrone N. Mercury as a global pollutant: sources, pathways, and effects. *Environ Sci Technol.* 2013;47(10):4967-4983.

2. Pirrone N, Cinnirella S, Feng X, Finkelman RB, Friedli HR, Leaner J, Mason R, Mukherjee AB, Stracher G, Streets DG *et al*: Global Mercury Emissions to the Atmosphere from Natural and Anthropogenic Sources. In: Mason R, Pirrone N, editors. *Mercury Fate and Transport in the Global Atmosphere: Emissions, Measurements and Models.* Boston, MA: Springer US;2009. p. 1-47.

3. Mason RP, Fitzgerald WF, Morel FMM. The Biogeochemical Cycling of Elemental Mercury - Anthropogenic Influences. *Geochimica Et Cosmochimica Acta.* 1994;58:3191-3198.

4. Barkay T, Miller SM, Summers AO. Bacterial mercury resistance from atoms to ecosystems. *FEMS Microbiol Rev.* 2003;27(2-3):355-384.

5. Crinnion WJ. Environmental medicine, part three: long-term effects of chronic low-dose mercury exposure. *Altern Med Rev.* 2000;5(3):209-223.

1104 6. Richardson GM, Wilson R, Allard D, Purtill C, Douma S, Graviere J. Mercury
1105 exposure and risks from dental amalgam in the US population, post-2000. *The*
1106 *Science of the total environment.* 2011;409(20):4257-4268.

1107 7. Diez S. Human health effects of methylmercury exposure. *Rev Environ Contam*
1108 *Toxicol.* 2009;198:111-132.

1109 8. Malm O. Gold mining as a source of mercury exposure in the Brazilian Amazon.
1110 *Environ Res.* 1998;77(2):73-78.

1111 9. Clarkson TW, Magos L. The toxicology of mercury and its chemical compounds.
1112 *Crit Rev Toxicol.* 2006;36(8):609-662.

1113 10. Hintelmann H, Hempel M, Wilken RD. Observation of unusual organic mercury
1114 species in soils and sediments of industrially contaminated sites. *Environ Sci*
1115 *Technol.* 1995;29(7):1845-1850.

1116 11. Tchounwou PB, Ayensu WK, Ninashvili N, Sutton D. Environmental exposure to
1117 mercury and its toxicopathologic implications for public health. *Environ Toxicol.*
1118 2003;18(3):149-175.

1119 12. Davidson PW, Myers GJ, Weiss B. Mercury exposure and child development
1120 outcomes. *Pediatrics.* 2004;113(Suppl 4):1023-1029.

1121 13. Valko M, Morris H, Cronin MT. Metals, toxicity and oxidative stress. *Curr Med*
1122 *Chem.* 2005;12(10):1161-1208.

1123 14. Yorifuji T, Tsuda T, Takao S, Harada M. Long-term exposure to methylmercury
1124 and neurologic signs in Minamata and neighboring communities. *Epidemiology.*
1125 2008;19(1):3-9.

1126 15. Zahir F, Rizwi SJ, Haq SK, Khan RH. Low dose mercury toxicity and human
1127 health. *Environ Toxicol Pharmacol.* 2005;20(2):351-360.

1128 16. Cheesman BV, Arnold AP, Rabenstein DL. Nuclear magnetic resonance studies of
1129 the solution chemistry of metal complexes. 25. Hg(thiol)3 complexes and HG(II)-
1130 thiol ligand exchange kinetics. *J Am Chem Soc.* 1988;110:6359-6364.

1131 17. Oram PD, Fang X, Fernando Q, Letkeman P, Letkeman D. The formation of
1132 constants of mercury(II)--glutathione complexes. *Chemical research in toxicology.*
1133 1996;9(4):709-712.

1134 18. Labunskyy VM, Hatfield DL, Gladyshev VN. Selenoproteins: molecular pathways
1135 and physiological roles. *Physiol Rev.* 2014;94(3):739-777.

1136 19. Pal PB, Pal S, Das J, Sil PC. Modulation of mercury-induced mitochondria-
1137 dependent apoptosis by glycine in hepatocytes. *Amino Acids.* 2012;42(5):1669-
1138 1683.

1139 20. Shenker BJ, Guo TL, Shapiro IM. Mercury-induced apoptosis in human lymphoid
1140 cells: evidence that the apoptotic pathway is mercurial species dependent. *Environ*
1141 *Res.* 2000;84(2):89-99.

1142 21. Jomova K, Valko M. Advances in metal-induced oxidative stress and human
1143 disease. *Toxicology.* 2011;283(2-3):65-87.

1144 22. Polacco BJ, Purvine SO, Zink EM, Lavoie SP, Lipton MS, Summers AO, Miller SM.
1145 Discovering mercury protein modifications in whole proteomes using natural
1146 isotope distributions observed in liquid chromatography-tandem mass
1147 spectrometry. *Mol Cell Proteomics.* 2011;10(8):M110.004853.

1148 23. LaVoie SP, Mapolelo DT, Cowart DM, Polacco BJ, Johnson MK, Scott RA, Miller
1149 SM, Summers AO. Organic and inorganic mercurials have distinct effects on
1150 cellular thiols, metal homeostasis, and Fe-binding proteins in Escherichia coli. *J*
1151 *Biol Inorg Chem.* 2015;20(8):1239-1251.

1152 24. McElwee MK, Ho LA, Chou JW, Smith MV, Freedman JH. Comparative
1153 toxicogenomic responses of mercuric and methyl-mercury. *BMC Genomics.*
1154 2013;14:698.

1155 25. Neidhardt FC, Bloch PL, Smith DF. Culture medium for enterobacteria. *J Bacteriol.*
1156 1974;119(3):736-747.

1157 26. Stead MB, Agrawal A, Bowden KE, Nasir R, Mohanty BK, Meagher RB, Kushner
1158 SR. RNAsnap: a rapid, quantitative and inexpensive, method for isolating total
1159 RNA from bacteria. *Nucleic acids research.* 2012;40(20):e156.

1160 27. Langmead B, Salzberg SL. Fast gapped-read alignment with Bowtie 2. *Nature*
1161 *methods.* 2012;9(4):357-359.

1162 28. Li H, Handsaker B, Wysoker A, Fennell T, Ruan J, Homer N, Marth G, Abecasis G,
1163 Durbin R, Genome Project Data Processing S. The Sequence Alignment/Map
1164 format and SAMtools. *Bioinformatics.* 2009;25(16):2078-2079.

1165 29. Anders S, Pyl PT, Huber W. HTSeq--a Python framework to work with high-
1166 throughput sequencing data. *Bioinformatics.* 2015;31(2):166-169.

1167 30. Hardcastle TJ, Kelly KA. baySeq: empirical Bayesian methods for identifying
1168 differential expression in sequence count data. *BMC bioinformatics.* 2010;11:422.

1169 31. Hamlett NV, Landale EC, Davis BH, Summers AO. Roles of the Tn21 merT, merP,
1170 and merC gene products in mercury resistance and mercury binding. *J Bacteriol.*
1171 1992;174(20):6377-6385.

1172 32. Summers AO, Lewis E. Volatilization of mercuric chloride by mercury-resistant
1173 plasmid-bearing strains of Escherichia coli, Staphylococcus aureus, and
1174 Pseudomonas aeruginosa. *J Bacteriol.* 1973;113(2):1070-1072.

1175 33. Summers AO, Silver S. Mercury resistance in a plasmid-bearing strain of
1176 Escherichia coli. *J Bacteriol.* 1972;112(3):1228-1236.

1177 34. Schaechter M, Santomassino KA. Lysis of Escherichia coli by sulfhydryl-binding
1178 reagents. *J Bacteriol.* 1962;84:318-325.

1179 35. Janssen BD, Hayes CS. The tmRNA ribosome-rescue system. *Adv Protein Chem*
1180 *Struct Biol.* 2012;86:151-191.

1181 36. Legendre P. Ward's Hierarchical Agglomerative Clustering Method: Which
1182 Algorithms Implement Ward's Criterion? *Journal of Classification.* 2014;31(3):274-
1183 295.

1184 37. Szklarczyk D, Franceschini A, Wyder S, Forslund K, Heller D, Huerta-Cepas J,
1185 Simonovic M, Roth A, Santos A, Tsafou KP *et al*. STRING v10: protein-protein
1186 interaction networks, integrated over the tree of life. *Nucleic acids research.*
1187 2015;43(Database issue):D447-452.

1188 38. von Mering C, Jensen LJ, Snel B, Hooper SD, Krupp M, Foglierini M, Jouffre N,
1189 Huynen MA, Bork P. STRING: known and predicted protein-protein associations,
1190 integrated and transferred across organisms. *Nucleic acids research.*
1191 2005;33(Database issue):D433-437.

1192 39. Arunasri K, Adil M, Khan PA, Shivaji S. Global gene expression analysis of long-
1193 term stationary phase effects in E. coli K12 MG1655. *PLoS One.*
1194 2014;9(5):e96701.

1195 40. Chang DE, Smalley DJ, Conway T. Gene expression profiling of Escherichia coli
1196 growth transitions: an expanded stringent response model. *Mol Microbiol.*
1197 2002;45(2):289-306.

1198 41. Kuzminov A. Recombinational repair of DNA damage in Escherichia coli and
1199 bacteriophage lambda. *Microbiol Mol Biol Rev.* 1999;63(4):751-813.

1200 42. Lusetti SL, Cox MM. The bacterial RecA protein and the recombinational DNA
1201 repair of stalled replication forks. *Annu Rev Biochem.* 2002;71:71-100.

1202 43. Salgado H, Martinez-Flores I, Lopez-Fuentes A, Garcia-Sotelo JS, Porron-Sotelo
1203 L, Solano H, Muniz-Rascado L, Collado-Vides J. Extracting regulatory networks of
1204 Escherichia coli from RegulonDB. *Methods Mol Biol.* 2012;804:179-195.

1205 44. Salgado H, Peralta-Gil M, Gama-Castro S, Santos-Zavaleta A, Muniz-Rascado L,
1206 Garcia-Sotelo JS, Weiss V, Solano-Lira H, Martinez-Flores I, Medina-Rivera A *et*
1207 *al*. RegulonDB v8.0: omics data sets, evolutionary conservation, regulatory
1208 phrases, cross-validated gold standards and more. *Nucleic acids research.*
1209 2013;41(Database issue):D203-213.

1210 45. Tramonti A, Visca P, De Canio M, Falconi M, De Biase D. Functional
1211 characterization and regulation of gadX, a gene encoding an AraC/XylS-like
1212 transcriptional activator of the Escherichia coli glutamic acid decarboxylase
1213 system. *J Bacteriol.* 2002;184(10):2603-2613.

1214 46. Nishino K, Senda Y, Yamaguchi A. The AraC-family regulator GadX enhances
1215 multidrug resistance in Escherichia coli by activating expression of mdtEF
1216 multidrug efflux genes. *J Infect Chemother.* 2008;14(1):23-29.

1217 47. Tucker DL, Tucker N, Ma Z, Foster JW, Miranda RL, Cohen PS, Conway T. Genes
1218 of the GadX-GadW regulon in Escherichia coli. *J Bacteriol.* 2003;185(10):3190-
1219 3201.

1220 48. Lemke JJ, Sanchez-Vazquez P, Burgos HL, Hedberg G, Ross W, Gourse RL.
1221 Direct regulation of Escherichia coli ribosomal protein promoters by the
1222 transcription factors ppGpp and DksA. *Proc Natl Acad Sci U S A.*
1223 2011;108(14):5712-5717.

1224 49. Nomura M, Gourse R, Baughman G. Regulation of the synthesis of ribosomes and
1225 ribosomal components. *Annu Rev Biochem.* 1984;53:75-117.

1226 50. Wilson DN, Nierhaus KH. The weird and wonderful world of bacterial ribosome
1227 regulation. *Crit Rev Biochem Mol Biol.* 2007;42(3):187-219.

1228 51. Soskine M, Steiner-Mordoch S, Schuldiner S. Crosslinking of membrane-
1229 embedded cysteines reveals contact points in the EmrE oligomer. *Proc Natl Acad*
1230 *Sci U S A.* 2002;99(19):12043-12048.

1231 52. Imesch E, Moosmayer M, Anner BM. Mercury weakens membrane anchoring of
1232 Na-K-ATPase. *The American journal of physiology.* 1992;262(5):F837-842.

1233 53. Carvalho CM, Chew EH, Hashemy SI, Lu J, Holmgren A. Inhibition of the human
1234 thioredoxin system. A molecular mechanism of mercury toxicity. *The Journal of*
1235 *biological chemistry.* 2008;283(18):11913-11923.

1236 54. Georgopoulos C, Welch WJ. Role of the major heat shock proteins as molecular
1237 chaperones. *Annu Rev Cell Biol.* 1993;9:601-634.

1238 55. Carpousis AJ. The RNA degradosome of Escherichia coli: an mRNA-degrading
1239 machine assembled on RNase E. *Annu Rev Microbiol.* 2007;61:71-87.

1240 56. Lim JY, May JM, Cegelski L. Dimethyl sulfoxide and ethanol elicit increased
1241 amyloid biogenesis and amyloid-integrated biofilm formation in Escherichia coli.
1242 *Appl Environ Microbiol.* 2012;78(9):3369-3378.

1243 57. Markarian SA, Poladyan AA, Kirakosyan GR, Trchounian AA, Bagramyan KA.
1244 Effect of diethylsulphoxide on growth, survival and ion exchange of Escherichia
1245 coli. *Lett Appl Microbiol.* 2002;34(6):417-421.

1246 58. Ansaldi M, Bordi C, Lepelletier M, Mejean V. TorC apocytochrome negatively
1247 autoregulates the trimethylamine N-oxide (TMAO) reductase operon in Escherichia
1248 coli. *Mol Microbiol.* 1999;33(2):284-295.

1249 59. Sorensen KI, Hove-Jensen B. Ribose catabolism of Escherichia coli:
1250 characterization of the rpiB gene encoding ribose phosphate isomerase B and of
1251 the rpiR gene, which is involved in regulation of rpiB expression. *J Bacteriol.*
1252 1996;178(4):1003-1011.

1253 60. Yamada T, Letunic I, Okuda S, Kanehisa M, Bork P. iPath2.0: interactive pathway
1254 explorer. *Nucleic acids research.* 2011;39(Web Server issue):W412-415.

1255 61. Imlay JA. The molecular mechanisms and physiological consequences of oxidative
1256 stress: lessons from a model bacterium. *Nat Rev Microbiol.* 2013;11(7):443-454.

1257 62. Grass G, Otto M, Fricke B, Haney CJ, Rensing C, Nies DH, Munkelt D. FieF (YiiP)
1258 from Escherichia coli mediates decreased cellular accumulation of iron and
1259 relieves iron stress. *Arch Microbiol.* 2005;183(1):9-18.

1260 63. Bandyopadhyay S, Chandramouli K, Johnson MK. Iron-sulfur cluster biosynthesis.
1261 *Biochem Soc Trans.* 2008;36(Pt 6):1112-1119.

1262 64. Johnson DC, Dean DR, Smith AD, Johnson MK. Structure, function, and formation
1263 of biological iron-sulfur clusters. *Annu Rev Biochem.* 2005;74:247-281.

1264 65. Rensing C, Mitra B, Rosen BP. The zntA gene of Escherichia coli encodes a Zn(II)-
1265 translocating P-type ATPase. *Proc Natl Acad Sci U S A.* 1997;94(26):14326-
1266 14331.

1267 66. Outten FW, Huffman DL, Hale JA, O'Halloran TV. The independent cue and cus
1268 systems confer copper tolerance during aerobic and anaerobic growth in
1269 Escherichia coli. *The Journal of biological chemistry.* 2001;276(33):30670-30677.

1270 67. Eitinger T, Mandrand-Berthelot MA. Nickel transport systems in microorganisms.
1271 *Arch Microbiol.* 2000;173(1):1-9.

1272 68. Qin J, Fu HL, Ye J, Bencze KZ, Stemmler TL, Rawlings DE, Rosen BP.
1273 Convergent evolution of a new arsenic binding site in the ArsR/SmtB family of
1274 metalloregulators. *The Journal of biological chemistry.* 2007;282(47):34346-34355.

1275 69. Alekshun MN, Levy SB. The mar regulon: multiple resistance to antibiotics and
1276 other toxic chemicals. *Trends Microbiol.* 1999;7(10):410-413.

1277 70. Nishino K, Yamada J, Hirakawa H, Hirata T, Yamaguchi A. Roles of TolC-
1278 dependent multidrug transporters of Escherichia coli in resistance to beta-lactams.
1279 *Antimicrob Agents Chemother.* 2003;47(9):3030-3033.

1280 71. Raetz CR, Reynolds CM, Trent MS, Bishop RE. Lipid A modification systems in
1281 gram-negative bacteria. *Annu Rev Biochem.* 2007;76:295-329.

1282 72. Checroun C, Gutierrez C. Sigma(s)-dependent regulation of yehZYXW, which
1283 encodes a putative osmoprotectant ABC transporter of Escherichia coli. *FEMS*
1284 *Microbiol Lett.* 2004;236(2):221-226.

1285 73. Van Houdt R, Michiels CW. Role of bacterial cell surface structures in Escherichia
1286 coli biofilm formation. *Res Microbiol.* 2005;156(5-6):626-633.

1287 74. Ma Q, Zhang G, Wood TK. Escherichia coli BdcA controls biofilm dispersal in
1288 Pseudomonas aeruginosa and Rhizobium meliloti. *BMC Res Notes.* 2011;4:447.

1289 75. Zhang XS, Garcia-Contreras R, Wood TK. YcfR (BhsA) influences Escherichia coli
1290 biofilm formation through stress response and surface hydrophobicity. *J Bacteriol.*
1291 2007;189(8):3051-3062.

1292 76. Itoh Y, Rice JD, Goller C, Pannuri A, Taylor J, Meisner J, Beveridge TJ, Preston
1293 JF, 3rd, Romeo T. Roles of pgaABCD genes in synthesis, modification, and export
1294 of the Escherichia coli biofilm adhesin poly-beta-1,6-N-acetyl-D-glucosamine. *J*
1295 *Bacteriol.* 2008;190(10):3670-3680.

1296 77. Lee J, Page R, Garcia-Contreras R, Palermino JM, Zhang XS, Doshi O, Wood TK,
1297 Peti W. Structure and function of the Escherichia coli protein YmgB: a protein
1298 critical for biofilm formation and acid-resistance. *J Mol Biol.* 2007;373(1):11-26.

1299 78. Cegelski L, Pinkner JS, Hammer ND, Cusumano CK, Hung CS, Chorell E, Aberg
1300 V, Walker JN, Seed PC, Almqvist F *et al*. Small-molecule inhibitors target
1301 Escherichia coli amyloid biogenesis and biofilm formation. *Nat Chem Biol.*
1302 2009;5(12):913-919.

1303 79. Seo SW, Kim D, Szubin R, Palsson BO. Genome-wide Reconstruction of OxyR
1304 and SoxRS Transcriptional Regulatory Networks under Oxidative Stress in
1305 Escherichia coli K-12 MG1655. *Cell Rep.* 2015;12(8):1289-1299.

1306 80. Choi H, Kim S, Mukhopadhyay P, Cho S, Woo J, Storz G, Ryu SE. Structural basis
1307 of the redox switch in the OxyR transcription factor. *Cell.* 2001;105(1):103-113.

1308 81. Altuvia S, Zhang A, Argaman L, Tiwari A, Storz G. The Escherichia coli OxyS
1309 regulatory RNA represses fhlA translation by blocking ribosome binding. *EMBO J.*
1310 1998;17(20):6069-6075.

1311 82. Amabile-Cuevas CF, Demple B. Molecular characterization of the soxRS genes of
1312 Escherichia coli: two genes control a superoxide stress regulon. *Nucleic acids*
1313 *research.* 1991;19(16):4479-4484.

1314 83. Greenberg JT, Monach P, Chou JH, Josephy PD, Demple B. Positive control of a
1315 global antioxidant defense regulon activated by superoxide-generating agents in
1316 Escherichia coli. *Proc Natl Acad Sci U S A.* 1990;87(16):6181-6185.

1317 84. Tsaneva IR, Weiss B. soxR, a locus governing a superoxide response regulon in
1318 Escherichia coli K-12. *J Bacteriol.* 1990;172(8):4197-4205.

1319 85. Watanabe S, Kita A, Kobayashi K, Miki K. Crystal structure of the [2Fe-2S]
1320 oxidative-stress sensor SoxR bound to DNA. *Proc Natl Acad Sci U S A.*
1321 2008;105(11):4121-4126.

1322 86. Keseler IM, Mackie A, Peralta-Gil M, Santos-Zavaleta A, Gama-Castro S,
1323 Bonavides-Martinez C, Fulcher C, Huerta AM, Kothari A, Krummenacker M *et al*.
1324 EcoCyc: fusing model organism databases with systems biology. *Nucleic acids*
1325 *research.* 2013;41(Database issue):D605-612.

1326 87. Anjem A, Varghese S, Imlay JA. Manganese import is a key element of the OxyR
1327 response to hydrogen peroxide in Escherichia coli. *Mol Microbiol.* 2009;72(4):844-
1328 858.

1329 88. Park SJ, Gunsalus RP. Oxygen, iron, carbon, and superoxide control of the
1330 fumarase fumA and fumC genes of Escherichia coli: role of the arcA, fnr, and soxR
1331 gene products. *J Bacteriol.* 1995;177(21):6255-6262.

1332 89. Varghese S, Tang Y, Imlay JA. Contrasting sensitivities of Escherichia coli
1333 aconitases A and B to oxidation and iron depletion. *J Bacteriol.* 2003;185(1):221-
1334 230.

1335 90. Eser M, Masip L, Kadokura H, Georgiou G, Beckwith J. Disulfide bond formation
1336 by exported glutaredoxin indicates glutathione's presence in the E. coli periplasm.
1337 *Proc Natl Acad Sci U S A.* 2009;106(5):1572-1577.

1338 91. Suzuki H, Koyanagi T, Izuka S, Onishi A, Kumagai H. The yliA, -B, -C, and -D
1339 genes of Escherichia coli K-12 encode a novel glutathione importer with an ATP-
1340 binding cassette. *J Bacteriol.* 2005;187(17):5861-5867.

1341 92. Vuilleumier S. Bacterial glutathione S-transferases: what are they good for? *J*
1342 *Bacteriol.* 1997;179(5):1431-1441.

1343 93. Summers AO, Wireman J, Vimy MJ, Lorscheider FL, Marshall B, Levy SB, Bennett
1344 S, Billard L. Mercury released from dental "silver" fillings provokes an increase in
1345 mercury- and antibiotic-resistant bacteria in oral and intestinal floras of primates.
1346 *Antimicrob Agents Chemother.* 1993;37(4):825-834.

1347 94. US - Food & Drug Administration (FDA): Mercury Levels in Commercial Fish and
1348 Shellfish (1990-2012)
1349 http://www.fda.gov/Food/FoodborneIllnessContaminants/Metals/ucm115644.htm

1350 95. McElwee MK, Freedman JH. Comparative toxicology of mercurials in
1351 Caenorhabditis elegans. *Environ Toxicol Chem.* 2011;30(9):2135-2141.

1352 96. Zheng M, Wang X, Templeton LJ, Smulski DR, LaRossa RA, Storz G. DNA
1353 microarray-mediated transcriptional profiling of the Escherichia coli response to
1354 hydrogen peroxide. *J Bacteriol.* 2001;183(15):4562-4570.

1355 97. Mehta HH, Liu Y, Zhang MQ, Spiro S. Genome-wide analysis of the response to
1356 nitric oxide in uropathogenic Escherichia coli CFT073. *Microb Genom.*
1357 2015;1(4):e000031.

1358 98. Rau MH, Calero P, Lennen RM, Long KS, Nielsen AT. Genome-wide Escherichia
1359 coli stress response and improved tolerance towards industrially relevant
1360 chemicals. *Microb Cell Fact.* 2016;15(1):176.

1361 99. Yung PY, Grasso LL, Mohidin AF, Acerbi E, Hinks J, Seviour T, Marsili E, Lauro
1362 FM. Global transcriptomic responses of Escherichia coli K-12 to volatile organic
1363 compounds. *Sci Rep.* 2016;6:19899.

1364 100. Wong GT, Bonocora RP, Schep AN, Beeler SM, Lee Fong AJ, Shull LM, Batachari
1365 LE, Dillon M, Evans C, Becker CJ *et al*. Genome-Wide Transcriptional Response
1366 to Varying RpoS Levels in Escherichia coli K-12. *J Bacteriol.* 2017;199(7).

1367 101. Ung CY, Lam SH, Hlaing MM, Winata CL, Korzh S, Mathavan S, Gong Z. Mercury-
1368 induced hepatotoxicity in zebrafish: in vivo mechanistic insights from transcriptome
1369 analysis, phenotype anchoring and targeted gene expression validation. *BMC*
1370 *Genomics.* 2010;11:212.

1371 102. Lash LH, Zalups RK. Alterations in renal cellular glutathione metabolism after in
1372 vivo administration of a subtoxic dose of mercuric chloride. *J Biochem Toxicol.*
1373 1996;11(1):1-9.

1374 103. Lu X, Xiang Y, Yang G, Zhang L, Wang H, Zhong S. Transcriptomic
1375 characterization of zebrafish larvae in response to mercury exposure. *Comp*
1376 *Biochem Physiol C Toxicol Pharmacol.* 2017;192:40-49.

1377 104. Kanai T, Takahashi K, Inoue H. Three distinct-type glutathione S-transferases from
1378 Escherichia coli important for defense against oxidative stress. *J Biochem.*
1379 2006;140(5):703-711.

1380 105. Xu FF, Imlay JA. Silver(I), mercury(II), cadmium(II), and zinc(II) target exposed
1381 enzymic iron-sulfur clusters when they toxify Escherichia coli. *Appl Environ*
1382 *Microbiol.* 2012;78(10):3614-3621.

1383 106. Varghese S, Wu A, Park S, Imlay KR, Imlay JA. Submicromolar hydrogen peroxide
1384 disrupts the ability of Fur protein to control free-iron levels in Escherichia coli. *Mol*
1385 *Microbiol.* 2007;64(3):822-830.

1386 107. Bagg A, Neilands JB. Ferric uptake regulation protein acts as a repressor,
1387 employing iron (II) as a cofactor to bind the operator of an iron transport operon in
1388 Escherichia coli. *Biochemistry.* 1987;26(17):5471-5477.

1389 108. de Lorenzo V, Wee S, Herrero M, Neilands JB. Operator sequences of the
1390 aerobactin operon of plasmid ColV-K30 binding the ferric uptake regulation (fur)
1391 repressor. *J Bacteriol.* 1987;169(6):2624-2630.

1392 109. Fontecave M, Choudens SO, Py B, Barras F. Mechanisms of iron-sulfur cluster
1393 assembly: the SUF machinery. *J Biol Inorg Chem.* 2005;10(7):713-721.

1394 110. Zhao G, Ceci P, Ilari A, Giangiacomo L, Laue TM, Chiancone E, Chasteen ND.
1395 Iron and hydrogen peroxide detoxification properties of DNA-binding protein from
1396 starved cells. A ferritin-like DNA-binding protein of Escherichia coli. *The Journal of*
1397 *biological chemistry.* 2002;277(31):27689-27696.

1398 111. Lund BO, Miller DM, Woods JS. Mercury-induced H2O2 production and lipid
1399 peroxidation in vitro in rat kidney mitochondria. *Biochem Pharmacol.* 1991;42
1400 Suppl:S181-187.

1401 112. Liochev SI, Fridovich I. Modulation of the fumarases of Escherichia coli in
1402 response to oxidative stress. *Arch Biochem Biophys.* 1993;301(2):379-384.

1403 113. Martin JE, Imlay JA. The alternative aerobic ribonucleotide reductase of
1404 Escherichia coli, NrdEF, is a manganese-dependent enzyme that enables cell
1405 replication during periods of iron starvation. *Mol Microbiol.* 2011;80(2):319-334.

1406 114. Jordan A, Aslund F, Pontis E, Reichard P, Holmgren A. Characterization of
1407 Escherichia coli NrdH. A glutaredoxin-like protein with a thioredoxin-like activity
1408 profile. *The Journal of biological chemistry.* 1997;272(29):18044-18050.

1409 115. Sharma SK, Goloubinoff P, Christen P. Heavy metal ions are potent inhibitors of
1410 protein folding. *Biochem Biophys Res Commun.* 2008;372(2):341-345.

1411 116. Arsene F, Tomoyasu T, Bukau B. The heat shock response of Escherichia coli. *Int*
1412 *J Food Microbiol.* 2000;55(1-3):3-9.

1413 117. Bissonnette SA, Rivera-Rivera I, Sauer RT, Baker TA. The IbpA and IbpB small
1414 heat-shock proteins are substrates of the AAA+ Lon protease. *Mol Microbiol.*
1415 2010;75(6):1539-1549.

1416 118. Gaubig LC, Waldminghaus T, Narberhaus F. Multiple layers of control govern
1417 expression of the Escherichia coli ibpAB heat-shock operon. *Microbiology.*
1418 2011;157(Pt 1):66-76.

1419 119. Matuszewska E, Kwiatkowska J, Kuczynska-Wisnik D, Laskowska E. Escherichia
1420 coli heat-shock proteins IbpA/B are involved in resistance to oxidative stress
1421 induced by copper. *Microbiology.* 2008;154(Pt 6):1739-1747.

1422 120. Wang A, Crowley DE. Global gene expression responses to cadmium toxicity in
1423 Escherichia coli. *J Bacteriol.* 2005;187(9):3259-3266.

1424 121. Salmon K, Hung SP, Mekjian K, Baldi P, Hatfield GW, Gunsalus RP. Global gene
1425 expression profiling in Escherichia coli K12. The effects of oxygen availability and
1426 FNR. *The Journal of biological chemistry.* 2003;278(32):29837-29855.

1427 122. Bibikov SI, Biran R, Rudd KE, Parkinson JS. A signal transducer for aerotaxis in
1428 Escherichia coli. *J Bacteriol.* 1997;179(12):4075-4079.

1429 123. Pruss BM, Campbell JW, Van Dyk TK, Zhu C, Kogan Y, Matsumura P. FlhD/FlhC
1430 is a regulator of anaerobic respiration and the Entner-Doudoroff pathway through
1431 induction of the methyl-accepting chemotaxis protein Aer. *J Bacteriol.*
1432 2003;185(2):534-543.

1433 124. Funk AE, Day FA, Brady FO. Displacement of zinc and copper from copper-
1434 induced metallothionein by cadmium and by mercury: in vivo and ex vivo studies.
1435 *Comp Biochem Physiol C.* 1987;86(1):1-6.

1436 125. O'Connor TR, Graves RJ, de Murcia G, Castaing B, Laval J. Fpg protein of
1437 Escherichia coli is a zinc finger protein whose cysteine residues have a structural
1438 and/or functional role. *The Journal of biological chemistry.* 1993;268(12):9063-
1439 9070.

1440 126. Binet MR, Poole RK. Cd(II), Pb(II) and Zn(II) ions regulate expression of the metal-
1441 transporting P-type ATPase ZntA in Escherichia coli. *FEBS Lett.* 2000;473(1):67-
1442 70.

1443 127. Petit-Hartlein I, Rome K, de Rosny E, Molton F, Duboc C, Gueguen E, Rodrigue A,
1444 Coves J. Biophysical and physiological characterization of ZraP from Escherichia
1445 coli, the periplasmic accessory protein of the atypical ZraSR two-component
1446 system. *Biochem J.* 2015;472(2):205-216.

1447 128. Colaco HG, Santo PE, Matias PM, Bandeiras TM, Vicente JB. Roles of Escherichia
1448 coli ZinT in cobalt, mercury and cadmium resistance and structural insights into the
1449 metal binding mechanism. *Metallomics.* 2016;8(3):327-336.

1450 129. Owens RA, Hartman PE. Export of glutathione by some widely used Salmonella
1451 typhimurium and Escherichia coli strains. *J Bacteriol.* 1986;168(1):109-114.

1452 130. Smirnova GV, Muzyka NG, Oktyabrsky ON. Effects of cystine and hydrogen
1453 peroxide on glutathione status and expression of antioxidant genes in Escherichia
1454 coli. *Biochemistry (Mosc).* 2005;70(8):926-934.

1455 131. Fitzgerald DM, Bonocora RP, Wade JT. Comprehensive mapping of the
1456 Escherichia coli flagellar regulatory network. *PLoS Genet.* 2014;10(10):e1004649.

132. Dong T, Yu R, Schellhorn H. Antagonistic regulation of motility and transcriptome expression by RpoN and RpoS in Escherichia coli. *Mol Microbiol.* 2011;79(2):375-386.

133. De Lay N, Gottesman S. A complex network of small non-coding RNAs regulate motility in Escherichia coli. *Mol Microbiol.* 2012;86(3):524-538.

134. Mermod M, Magnani D, Solioz M, Stoyanov JV. The copper-inducible ComR (YcfQ) repressor regulates expression of ComC (YcfR), which affects copper permeability of the outer membrane of Escherichia coli. *Biometals.* 2012;25(1):33-43.

135. Schwechheimer C, Kuehn MJ. Outer-membrane vesicles from Gram-negative bacteria: biogenesis and functions. *Nat Rev Microbiol.* 2015;13(10):605-619.

136. Crepin S, Chekabab SM, Le Bihan G, Bertrand N, Dozois CM, Harel J. The Pho regulon and the pathogenesis of Escherichia coli. *Vet Microbiol.* 2011;153(1-2):82-88.

137. Hsieh YJ, Wanner BL. Global regulation by the seven-component Pi signaling system. *Curr Opin Microbiol.* 2010;13(2):198-203.

138. Hondorp ER, Matthews RG. Oxidative stress inactivates cobalamin-independent methionine synthase (MetE) in Escherichia coli. *PLoS Biol.* 2004;2(11):e336.

139. Brooks P, Davidson N. Mercury(II) Complexes of Imidazole and Histidine. *Journal of the American Chemical Society.* 1960;82(9):2118-2123.

140. Pal C, Bengtsson-Palme J, Kristiansson E, Larsson DG. Co-occurrence of resistance genes to antibiotics, biocides and metals reveals novel insights into their co-selection potential. *BMC Genomics.* 2015;16(1):964.

141. Wireman J, Liebert CA, Smith T, Summers AO. Association of mercury resistance with antibiotic resistance in the gram-negative fecal bacteria of primates. *Appl Environ Microbiol.* 1997;63(11):4494-4503.

142. Mehta P, Casjens S, Krishnaswamy S. Analysis of the lambdoid prophage element e14 in the E. coli K-12 genome. *BMC Microbiol.* 2004;4:4.

143. Wang X, Kim Y, Ma Q, Hong SH, Pokusaeva K, Sturino JM, Wood TK. Cryptic prophages help bacteria cope with adverse environments. *Nat Commun.* 2010;1:147.

1489 **Table 1: Genes with ≥ 20 fold-change for at least two time points after $HgCl_2$ exposure (n = 25).**

Gene ID	Gene Name	Product Description	Hg t10	Hg t30	Hg t60	PMA t10	PMA t30	PMA t60
b1112	**bhsA**	Biofilm, cell surface and signaling defects, YhcN family	**1949**	**563**	**94**	**46**	**21**	n.s.
b4458	oxyS	OxyS sRNA activates genes that detoxify oxidative damage	**1524**	**1292**	**150**	10	6	n.s.
b4249	bdcA	c-di-GMP-binding biofilm dispersal mediator protein	**596**	**79**	7	16	2	n.s.
b3686	**ibpB**	Chaperone, heat-inducible protein of HSP20 family	**402**	**124**	**281**	**37**	**211**	9
b0812	dps	Stress-induced Fe-binding and storage protein	**339**	**52**	n.s.	4	2	n.s.
b4248	yjgH	Putative reactive intermediate deaminase, UPF0076 family	**296**	**24**	3	6	2	n.s.
b0849	grxA	Glutaredoxin 1	**246**	**33**	n.s.	14	4	n.s.
b1144	ymfJ	Function unknown, e14 prophage	**185**	**39**	n.s.	3	3	n.s.
b2582	**trxC**	Thioredoxin 2, zinc-binding; Trx2	**134**	**50**	7	**24**	**24**	n.s.
b1147	ymfL*	Function unknown, e14 prophage	**95**	**29**	n.s.	n.s.	3	n.s.
b1146	croE*	Cro-like repressor, e14 prophage	**90**	**40**	n.s.	n.s.	n.s.	n.s.
b3687	**ibpA**	Chaperone, heat-inducible protein of HSP20 family	**86**	19	**41**	10	**28**	4
b2531	iscR	Transcriptional repressor for isc operon; contains Fe-S cluster	**62**	**48**	9	12	18	n.s.
b1148	ymfM*	Function unknown, e14 prophage	**49**	**21**	n.s.	n.s.	n.s.	n.s.
b4599	yneM	function unknown, membrane-associated; regulated by PhoPQ	**38**	**36**	n.s.	3	3	n.s.
b2673	nrdH	NrdH-redoxin reducing oxidized NrdEF	**35**	**127**	**21**	7	14	n.s.
b4030	**psiE**	Pho regulon, regulated by phoB and cAMP	**35**	**64**	17	**38**	**59**	n.s.
b1684	sufA	Scaffold protein for assembly of iron-sulfur clusters	**32**	**39**	5	n.s.	3	n.s.
b1748	**astC**	Succinylornithine transaminase; carbon starvation protein	**30**	**31**	**25**	**34**	**36**	n.s.
b4663	**azuC**	Function unknown; membrane-associated	**27**	**25**	**36**	**41**	**49**	n.s.
b0484	copA	Copper-, silver-translocating P-type ATPase efflux pump	**25**	**20**	n.s.	5	n.s.	-10
b2674	nrdI	Flavodoxin required for NrdEF cluster assembly	**21**	**73**	**22**	4	7	n.s.
b1747	astA*	Arginine succinyltransferase, arginine catabolism	10	**20**	**29**	9	14	n.s.
b1020	**phoH**	ATP-binding protein, function unknown	8	**71**	**221**	**61**	**365**	n.s.
b4002	zraP	Zn-dependent periplasmic chaperone	3	**27**	**43**	n.s.	n.s.	-3

1490

1491 Table is sorted by Hg at 10 min column. n.s. = not significantly different from unexposed culture and boldface highlights actual values ≥

1492 20-fold. Gene names in boldface have a ≥ 20 differential expression response to both Hg and PMA in at least one time point (n = 8). Genes

1493 marked with an asterisk (*) had fewer than 11 average read counts for at least 2 time points in the unexposed condition and were

1494 operationally defined as being "off" in that condition. Such genes constituted, the lowest 15th percentile of all genes, based on raw read

1495 counts normalized across all libraries and across all biological replicates.

1496 **Table 2: Genes with ≥ 20 fold-change in at least two time points for PMA exposure (n= 17).**

Gene ID	Gene Name	Product Description	Hg t10	Hg t30	Hg t60	PMA t10	PMA t30	PMA t60
b3728	pstS	ABC phosphate transport system; periplasmic binding protein	n.s.	16	8	**86**	**165**	n.s.
b1020	**phoH**	ATP-binding protein, function unknown	8	**71**	**221**	**61**	**365**	n.s.
b0996	torC*	c-Type cytochrome	n.s.	n.s.	n.s.	**55**	**65**	**77**
b4060	**yjcB**	Function unknown	**33**	11	12	**52**	**35**	n.s.
b0399	**phoB**	Positive response regulator for pho regulon	4	**22**	3	**51**	**105**	n.s.
b1530	**marR**	Transcription repressor of multiple antibiotic resistance	**26**	7	n.s.	**48**	**29**	n.s.
b1531	marA	Transcriptional activator for multiple antibiotic resistance;	15	9	n.s.	**46**	**31**	n.s.
b1112	**bhsA**	Biofilm, cell surface and signaling defects, YhcN family	**1949**	**563**	**94**	**46**	**21**	n.s.
b1532	marB	marRAB multiple antibiotic resistance operon	16	8	n.s.	**45**	**27**	n.s.
b4663	**azuC**	Function unknown; membrane-associated	**27**	**25**	**36**	**41**	**49**	n.s.
b4030	**psiE**	Pho regulon, regulated by phoB and cAMP	**35**	**64**	17	**38**	**59**	n.s.
b3686	**ibpB**	Chaperone, heat-inducible protein of HSP20 family	**402**	**124**	**281**	**37**	**211**	9
b1748	**astC**	Succinylornithine transaminase; carbon starvation protein	**30**	**31**	**25**	**34**	**36**	n.s.
b3469	**zntA**	Zn(II), Cd(II), and Pb(II) translocating P-type ATPase	**40**	19	8	**29**	**22**	n.s.
b2582	**trxC**	Thioredoxin 2, zinc-binding; Trx2	**134**	**50**	7	**24**	**24**	n.s.
b4354	yjiY	Predicted transporter, function unknown	n.s.	n.s.	n.s.	**20**	**77**	n.s.
b1625	cnu	OriC-binding complex H-NS/Cnu	n.s.	10	n.s.	**20**	**24**	n.s.

1497

1498 Table is sorted by PMA at 10 min column. n.s. = not significantly different from unexposed culture and boldface highlights actual values ≥
1499 20-fold. Gene names in boldface have a ≥ 20 differential expression response to both Hg and PMA in at least one time point (n = 11).
1500 Genes marked with an asterisk (*) had fewer than 11 average read counts for at least 2 time points in the unexposed condition and were
1501 operationally defined as being "off" in that condition. Such genes constituted, the lowest 15th percentile of all genes, based on raw read
1502 counts normalized across all libraries and across all biological replicates.

1503

1504 **Table 3: Changes in transcription factor gene expression.** The sum of transcription

1505 factor genes either up-regulated or down-regulated is shown with the percentage of the

1506 total transcription factor genes in parenthesis; percents do not total 100 because genes

1507 with no change compared to unexposed cells are not tabulated here. See details in

1508 Table S12.

1509

Transcription Factors (n = 203)						
	Hg_t10	**Hg_t30**	**Hg_t60**	**PMA_t10**	**PMA_t30**	**PMA_t60**
up	63 (31)	46 (23)	14 (7)	86 (42)	78 (38)	1 (0.5)
down	28 (14)	28 (14)	13 (6)	22 (11)	23 (11)	2 (1)

1510

1511

1512

1513

1514

1515

1516

1517

1518

1519

1520

1521

1522

1523

1524

1525 **Figures**

1526

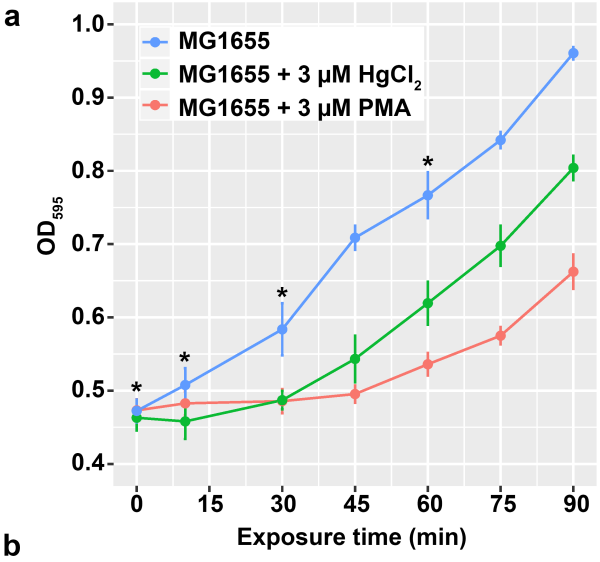

	t10	t30	t60
3 μM $HgCl_2$	1,821 (894↑927↓)	1,422 (637↑785↓)	563 (259↑304↓)
3 μM PMA	2,181 (1,261↑920↓)	2,009 (1,156↑853↓)	65 (36↑29↓)

1527

1528 **Figure 1: Effects of sub-acute mercury exposure on growth of MG1655. (a)** *E. coli*
1529 K12 MG1655 grown in MOPS minimal medium, unexposed (blue) or exposed to 3 μM
1530 $HgCl_2$ (red) or 3 μM PMA (green) during mid-log phase. Asterisks indicate sampling
1531 times for RNA-seq. Error bars are standard error (SEM) of 3 biological replicates for
1532 each culture condition. See Figure S1 for full growth curve. **(b)** Significantly differentially
1533 expressed genes (DEG) counts (up-regulated or down-regulated) for $HgCl_2$ and PMA
1534 relative to unexposed control culture at each time point.

1535

1536

1537

1538

1539

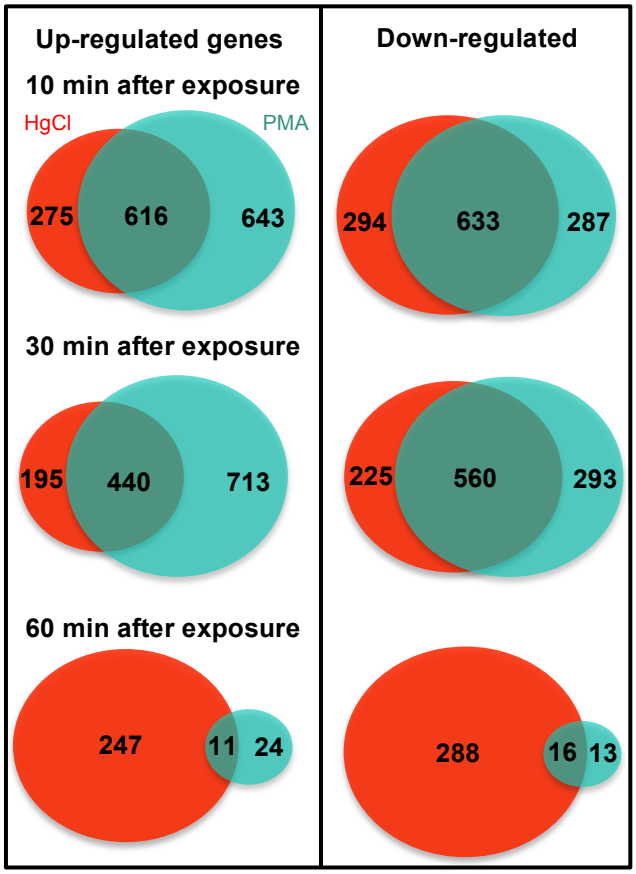

1540

1541

1542 **Figure 2: Overlap between differentially expressed genes at each sampling time**

1543 The 3 μM $HgCl_2$ exposure is in red and the 3 μM PMA exposure in green. Ovals are to

1544 scale only at each time point, but not between between time points in a panel nor

1545 between left and right panels.

1546

1547

1548

1549

1550

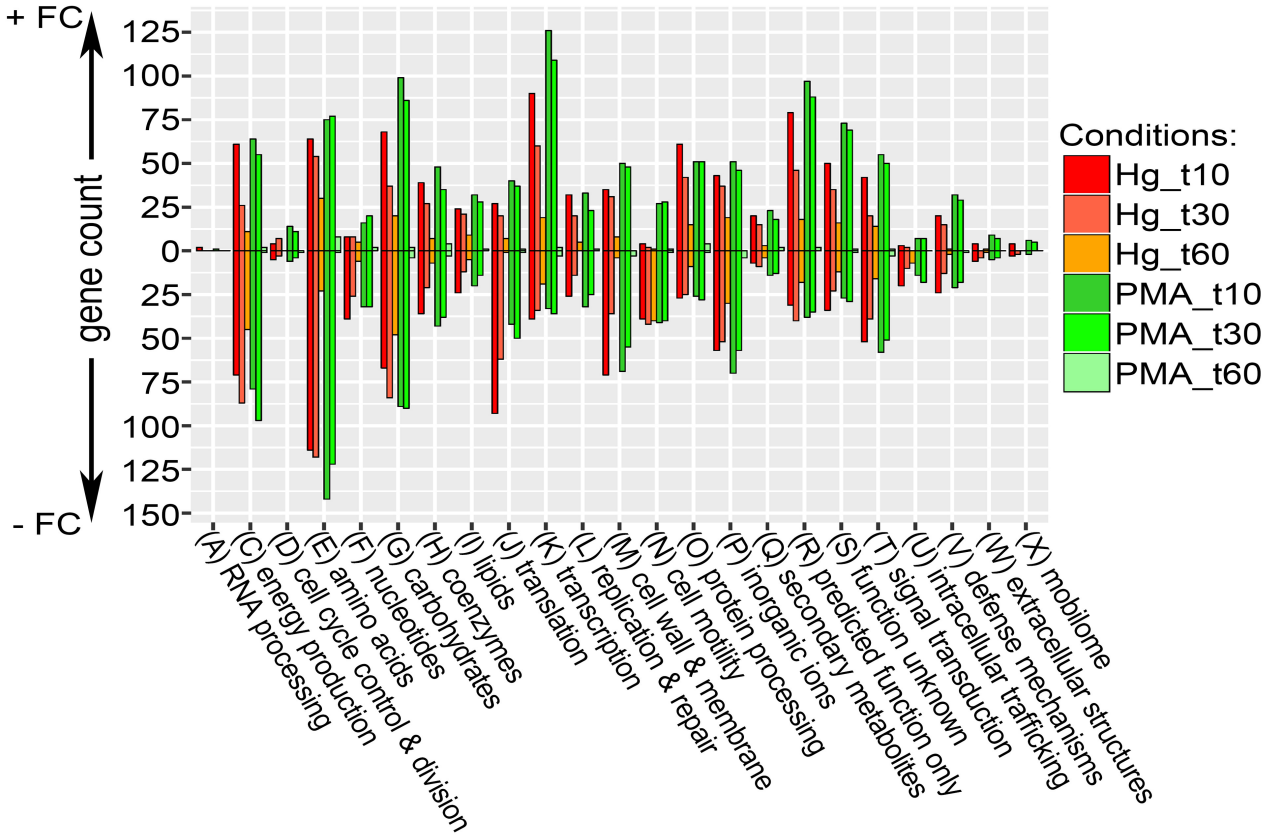

Figure 3: Counts of differentially expressed genes for each condition grouped by COG functional category. Genes with a $\log_2$ fold-change ≥ 1 for each condition were grouped by COG group. Positive counts represent observed up-regulated genes and negative counts represent observed down-regulated genes. COG code, number of proteins encoded by genome and category description: (A, 2) RNA processing and modification; (C, 284) Energy production and conversion; (D, 39) Cell cycle control, cell division, chromosome partitioning; (E, 355) Amino acid transport and metabolism; (F, 107) Nucleotide transport and metabolism; (G, 381) Carbohydrate transport and metabolism; (H, 179) Coenzyme transport and metabolism; (I, 121) Lipid transport and

1563 metabolism; (J, 236) Translation, ribosomal structure and biogenesis; (K, 294)
1564 Transcription; (L, 139) Replication, recombination and repair; (M, 242) Cell wall,
1565 membrane and envelope biogenesis; (N, 102) Cell motility; (O, 156) Post-translational
1566 modification, protein turnover, chaperones; (P, 223) Inorganic ion transport and
1567 metabolism; (Q, 68) Secondary metabolites biosynthesis, transport and catabolism; (R,
1568 261) General function prediction only; (S, 203) Function unknown; (T, 191) Signal
1569 transduction mechanisms; (U, 50) Intracellular trafficking, secretion, and vesicular
1570 transport; (V, 91) Defense mechanisms; (W, 31) Extracellular structures; (X, 60)
1571 Mobilome, prophages, transposons.
1572
1573
1574
1575
1576
1577
1578
1579
1580
1581
1582
1583
1584
1585

1586

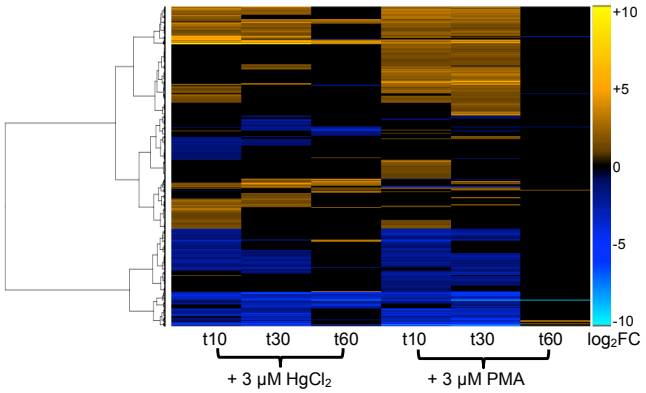

1587

1588

1589 **Figure 4: Differentially expressed genes at each RNA sampling time.** Heat map of

1590 all genes that were differentially expressed in at least one mercury exposure condition

1591 (n = 3,149). Genes were clustered by row using Ward's minimum variance method [36]

1592 with non-squared $\log_2$ fold-change input values.

1593

1594

1595

1596

1597

1598

1599

1600

1601

1602

1603

1604

1605

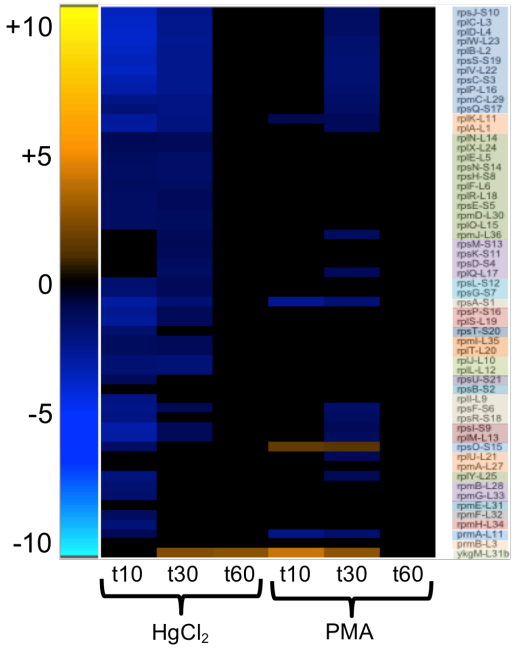

1606

1607

1608 **Figure 5: Ribosomal subunit protein genes.** Genes are grouped and colored by

1609 operon (see larger Figure S11 and Table S13 for details).

1610

1611

1612

1613

1614

1615

1616

1617

1618

1619

1620

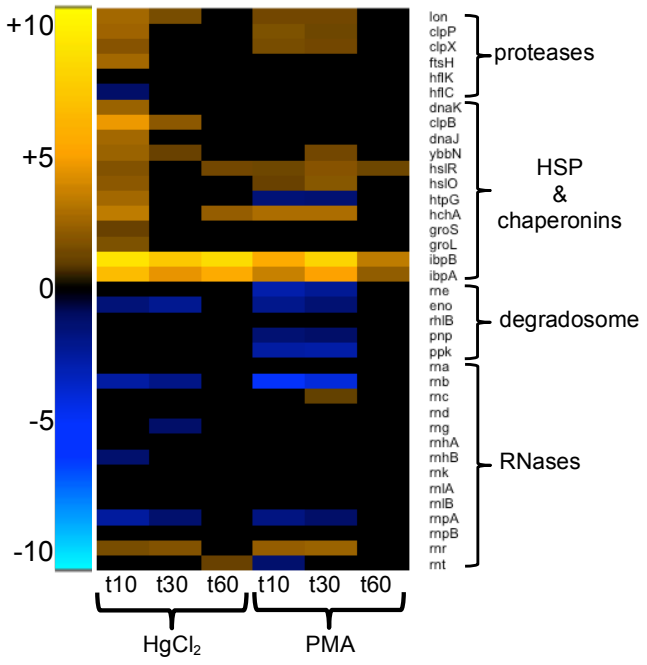

1621

1622

1623 **Figure 6: Protein and RNA turnover and repair**. (see larger Figure S12 and Table

1624 S13 for details).

1625

1626

1627

1628

1629

1630

1631

1632

1633

1634

1635

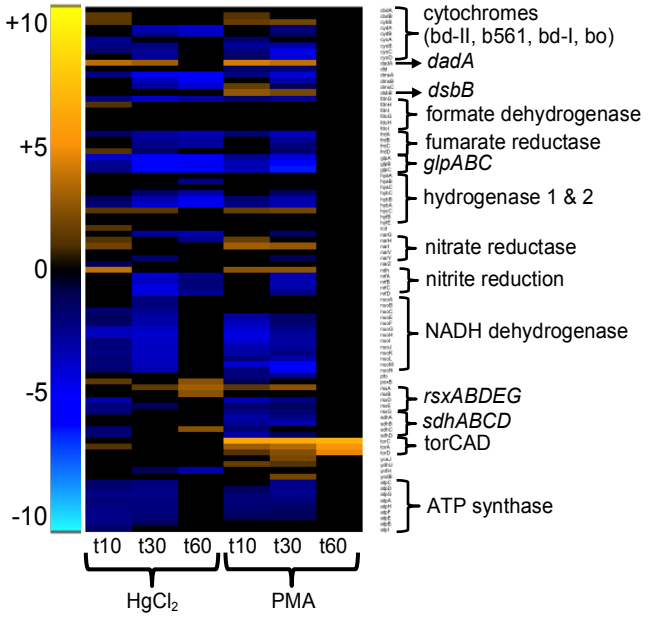

1636

1637

1638 **Figure 7: Electron transport chain and ATP-synthase.** (see larger Figure S13 and

1639 Table S13 for details).

1640

1641

1642

1643

1644

1645

1646

1647

1648

1649

1650

1651

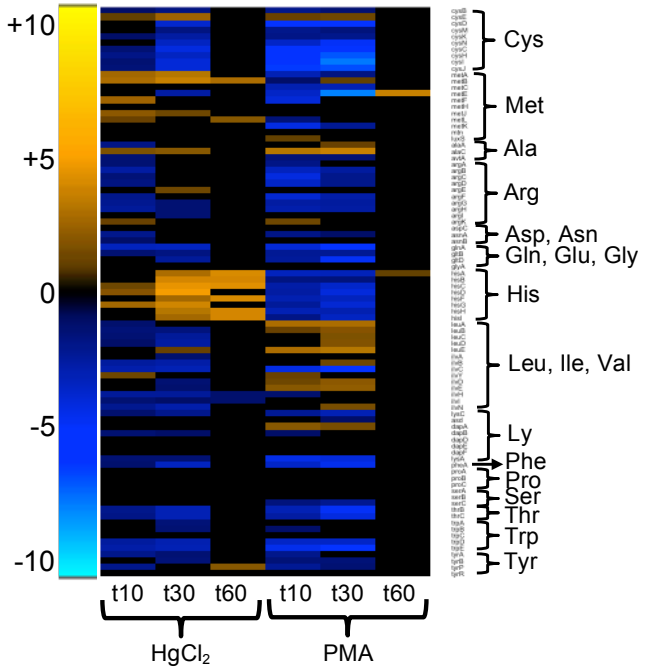

1652

1653

1654 **Figure 8: Amino acid biosynthesis.** (see larger Figure S22 and Table S13 for details).

1655

1656

1657

1658

1659

1660

1661

1662

1663

1664

1665

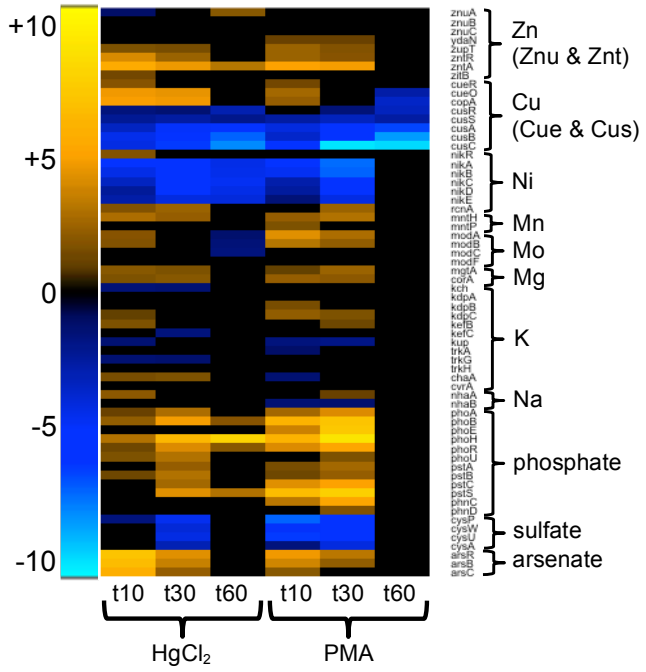

Figure 9: Non-ferrous metals homeostases. (see larger Figure S23 and Table S13 for details).

1681

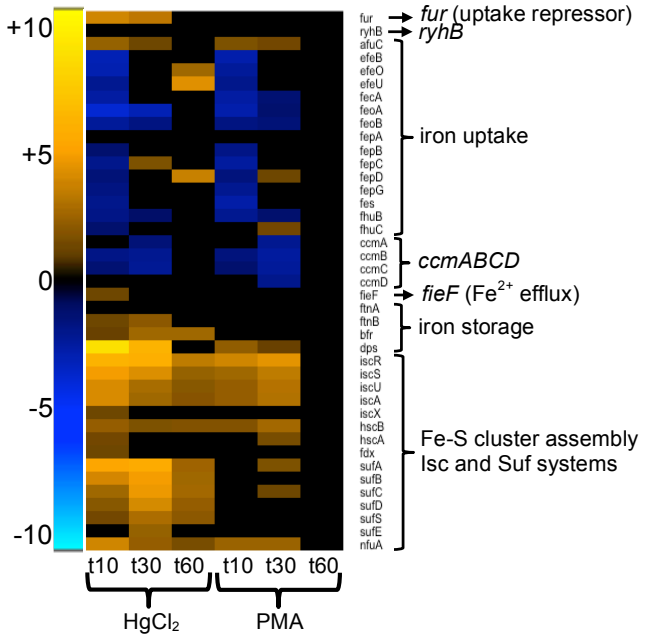

1682

1683

1684 **Figure 10: Iron homeostasis.** (see larger Figure S24 and Table S13 for details).

1685

1686

1687

1688

1689

1690

1691

1692

1693

1694

1695

1696

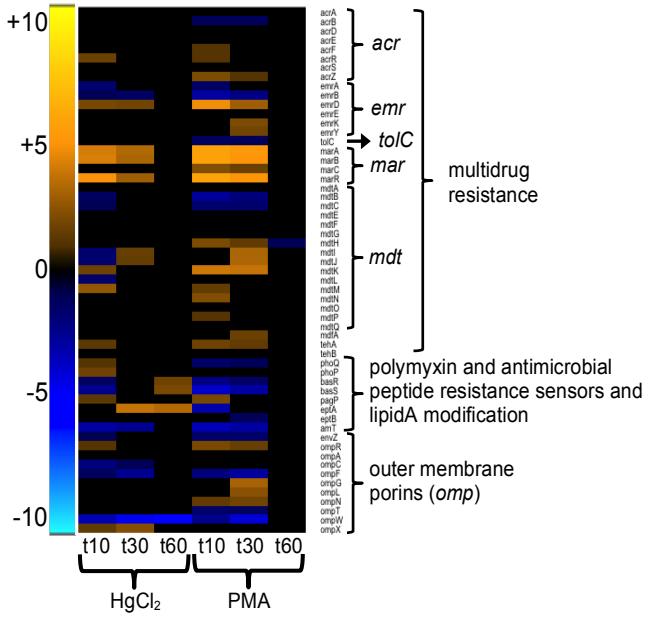

1697

1698

1699 **Figure 11: Antibiotic resistance and outer membrane porins.** (see larger Figure S26

1700 and Table S13 for details).

1701

1702

1703

1704

1705

1706

1707

1708

1709

1710

1711

1712

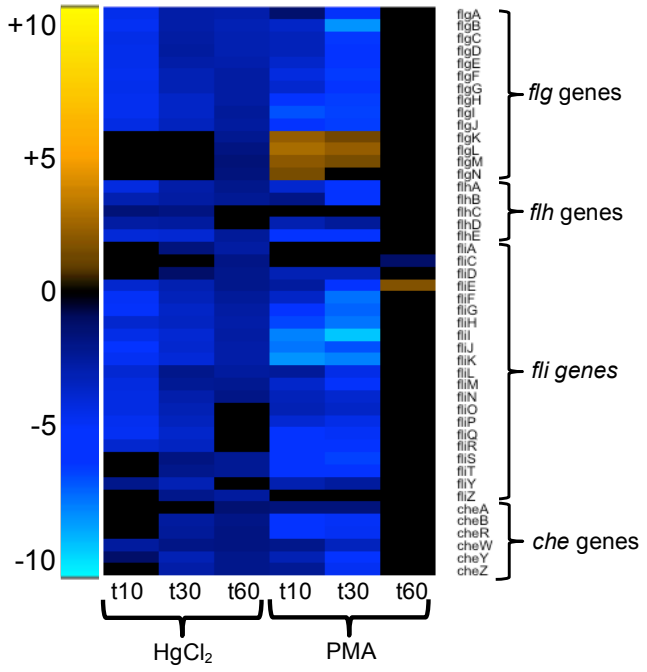

1713

1714

1715 **Figure 12: Flagella components and chemotaxis.** (see larger Figure S27 and Table

1716 S13 for details).

1717

1718

1719

1720

1721

1722

1723

1724

1725

1726

1727

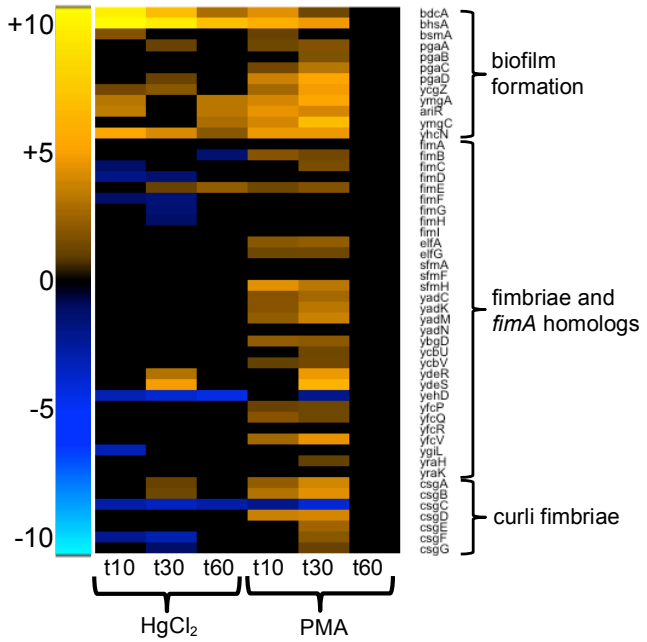

1728

1729

1730 **Figure 13: Biofilm formation and fimbriae.** (see larger Figure S28 and Table S13 for

1731 details).

1732

1733

1734

1735

1736

1737

1738

1739

1740

1741

1742

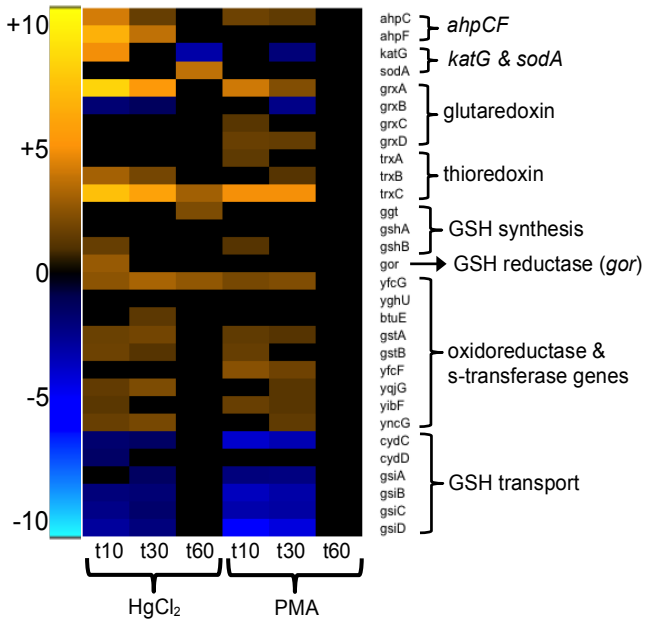

1743

1744

1745 **Figure 14: Oxidative stress defense and thiol homeostases.** (see larger Figure S29

1746 and Table S13).

1747

1748

1749

1750

1751

1752

1753

1754

1755

1756

1757